HHS Public Access

Author manuscript

J Immunol. Author manuscript; available in PMC 2020 October 15.

Published in final edited form as:

J Immunol. 2019 October 15; 203(8): 2239–2251. doi:10.4049/jimmunol.1701686.

Glutathione Reductase Promotes Fungal Clearance and Suppresses Inflammation during Systemic *Candida albicans* Infection in Mice

Victoria Y. Kim[*], **Abel Batty**[*], **Jinhui Li**[*], **Sean G. Kirk**[*], **Yi Jin**[*], **Juan Tang**[†], **Jian Zhang**[‡], **Lynette K. Rogers**[*,¶], **Han-Xiang Deng**[§], **Leif D. Nelin**[*,¶], **Yusen Liu**[*,¶,‖]

[*]Center for Perinatal Research, The Abigail Wexner Research Institute at Nationwide Children's Hospital, Columbus, Ohio, United States of America

[†]Department of Microbial Infection and Immunity, The Ohio State University, Columbus, Ohio, United States of America

[‡] Department of Pathology, University of Iowa Carver College of Medicine, Iowa City, Iowa, United States of America

[§]Ken and Ruth Davee Department of Neurology, Northwestern University Feinberg School of Medicine, Chicago, Illinois, USA.

[¶]Department of Pediatrics, The Ohio State University College of Medicine, Columbus, Ohio, United States of America

Abstract

Glutathione reductase (Gsr)[1] catalyzes the reduction of glutathione disulfide (GSSG) to glutathione (GSH), which plays an important role in redox regulation. We have previously shown that Gsr facilitates neutrophil bactericidal activities and is pivotal for host defense against bacterial pathogens. However, it is unclear whether Gsr is required for immune defense against fungal pathogens. It is also unclear whether Gsr plays a role in immunological functions outside of neutrophils during immune defense. In this study, we report that *Gsr*$^{-/-}$ mice exhibited markedly increased susceptibility to *C. albicans* challenge. Upon *C. albicans* infection, *Gsr*$^{-/-}$ mice exhibited dramatically increased fungal burden in the kidneys, cytokine and chemokine storm, striking neutrophil infiltration and histological abnormalities in both the kidneys and hearts, and substantially elevated mortality. Large fungal foci surrounded by massive numbers of neutrophils were detected outside of the glomeruli in the kidneys of *Gsr*$^{-/-}$ mice but were not found in wildtype mice. Examination of the neutrophils and macrophages of *Gsr*$^{-/-}$ mice revealed several defects. *Gsr*$^{-/-}$ neutrophils exhibited compromised phagocytosis, attenuated respiratory burst, and

[1]Abbreviations used in this article: Gsr, glutathione reductase; ADHP, 10-acetyl-3,7-dihydroxyphenoxazine; BM, bone marrow; BMDM, bone marrow-derived macrophages; CLR, C-type lectin receptor; GSH, glutathione; GSSG, glutathione disulfide; ITAM, immunoreceptor tyrosine activation motif; MK2, MAPK-Activated protein kinase-2; Mkp-1, mitogen-activated protein kinase phosphatase-1; MOI, multiplicity of infection; MPO, myeloperoxidase; NLR, nucleotide oligomerization domain-like receptor; PAS, periodic acid-Schiff; ROS, reactive oxygen species.

[‖]Address correspondence and reprint requests to Professor Yusen Liu, Center for Perinatal Research, The Abigail Wexner Research Institute at Nationwide Children's Hospital, 575 Children's Cross Road, Columbus, OH 43215. yusen.liu@nationwidechildrens.org.

Disclosures

The authors have no financial conflicts of interest.

impaired fungicidal activity *in vitro*. Moreover, upon *C. albicans* stimulation, $Gsr^{-/-}$ macrophages produced increased levels of inflammatory cytokines and exhibited elevated p38 and JNK activities, at least in part due to lower mitogen-activated protein kinase phosphatase (Mkp)-1 activity and greater Syk activity. Thus, Gsr-mediated redox regulation is crucial for fungal clearance by neutrophils and the proper control of the inflammatory response by macrophages during host defense against fungal challenge.

Introduction

Candida species are the fourth most common cause of nosocomial infections according to the CDC (1), and it is estimated that approximately 46,000 cases of healthcare-associated invasive candidiasis occur each year in the U.S. (2, 3). Candidemia is one of the most common blood stream infections in the US (4–6). *C. albicans* accounts for 51% of the nosocomial Candida blood stream infections (4, 7). Thus, there is an urgent need to understand the immune defense against *C. albicans*. Invasive *C. albicans*, in both the yeast and hypha forms, trigger a strong immune defense through pattern recognition receptors on innate immune cells such as macrophages and epithelial cells, including TLRs, the C-type lectin receptors (CLRs), and the nucleotide oligomerization domain-like receptors (NLRs) (8). Dectin-1, the most well-studied CLRs in monocytes and macrophages, recognizes *C. albicans* β-glucans and is involved in both the ligand uptake and phagocytosis (9–11). Engagement of β-glucans with Dectin-1 triggers tyrosine phosphorylation of an immunoreceptor tyrosine activation (ITAM)-like motif, which in turn recruits and activates the Syk tyrosine kinase, leading to activation of both NF-κB and MAPKs through a signaling pathway mediated by Card9 and Raf (9, 12–14). Dectin-2 and Dectin-3 recognize α-mannan-rich structures of *C. albicans* (9, 15, 16). Unlike Dectin-1, which has an ITAM-like motif, Dectin-2 and -3 do not have an ITAM-like motif (16, 17). Instead, recognition of α-mannans by Dectin-2 and -3 triggers tyrosine phosphorylation of the ITAM motif of FcγR to induce Syk activation and the subsequent NF-κB and MAPK cascades (15, 17). In addition to CLRs, TLRs and NLRs also recognize ligands of *C. albicans* and elicit multiple signal transduction pathways, ultimately leading to activation of NF-κB and MAPKs (8, 9, 17).

NF-κB regulates the transcription of a myriad of inflammatory cytokine and chemokine genes, including TNF-α, IL-1β, and IL-6, while MAPKs, particularly p38, enhance both the stability and the translation of cytokine and chemokine mRNAs. Mice deficient in TNF-α are highly susceptible to *C. albicans* infection, highlighting the crucial role of this cytokine in anti-fungal host defense (18). These inflammatory cytokines and chemokines are crucial in the recruitment of neutrophils, the most important leukocytes in the elimination of *C. albicans*. IL-6 is critical for the development of Th-17 cell-mediated adaptive immunity, which also mobilizes neutrophils against *C. albicans* (19, 20). Upon encountering *C. albicans*, neutrophils can engulf the fungal pathogens into the phagosomes through phagocytosis (21). The most important anti-microbial arsenal of neutrophils is the production of microbicidal reactive oxygen species (ROS) through the NADPH oxidase-mediated respiratory burst (21). The phagosomal respiratory burst is initiated by a stimulus-dependent assembly of the NADPH oxidase complex after phagocytosis of microbial

pathogens (22, 23). Respiratory burst triggered by microbial particulates starts with recruitment of cytosolic NADPH oxidase subunits, including $p47^{phox}$, $p40^{phox}$, $p67^{phox}$, and Rac2 GTPase to the membrane-associated $gp91^{phox}$ and $p22^{phox}$ subunits (23). A number of cell signaling regulators have been shown to mediate NADPH oxidase activation in neutrophils, including Syk, PKC, and ERK and p38 MAPKs (24–27). In the phagosome membrane, NADPH oxidase reduces molecular oxygen to yield $O_2^{\bullet -}$, which dismutes to produce H_2O_2. Myeloperoxidase (MPO) released from azurophilic granules catalyzes the conversion of H_2O_2 and Cl^- to the highly bactericidal hypochlorous acid in the phagolysosomes (21). The fact that chronic granulomatous disease patients with defects in respiratory burst are susceptible to fungal infections highlights the critical role of respiratory burst in antifungal immune defense (28).

GSH is a major cellular antioxidant, which protects cells from oxidative damage. In the cytosol, GSH reacts with H_2O_2 and is oxidized to GSSG (29, 30). Gsr catalyzes the regeneration of GSH from GSSG (GSSG + NADPH + $H^+ \rightarrow$ 2GSH + $NADP^+$), utilizing NADPH as an electron donor. Therefore, it is thought that during infections Gsr functions to protect neutrophils from oxidative damage through perpetuating the GSH/GSSG cycle that eliminates harmful H_2O_2 in the cytosol (29). Earlier studies using neutrophils from GSR-deficient patients have demonstrated a critical role of GSR in the neutrophil respiratory burst (31). However, since no overt increase in susceptibility to infections was reported in these GSR-deficient patients (30, 32, 33), the functional importance of GSR in host defense was unclear. Previously, we have studied the effects of Gsr deficiency on host defense against bacterial pathogen using a mouse model of sepsis (34, 35). We have demonstrated that Gsr is crucial for host defense against *Escherichia coli*, *Staphylococcus aureus*, and group B Streptococcal infections by facilitating neutrophil respiratory burst and the generation of neutrophil extracellular traps (34, 35). It remains unclear how Gsr deficiency affects host defense against fungal pathogens and whether Gsr functions in phagocytic cells other than neutrophils. In the present studies, we addressed these questions using *Gsr*-deficient mice and *C. albicans* fungal pathogen. Our studies demonstrated that Gsr is crucial for host defense against *C. albicans*, facilitating *C. albicans* killing by neutrophils and restraining TNF-α production *via* attenuation of Syk activity and MAPK pathways in macrophages.

Materials and Methods

Reagents

Rabbit antibodies against phospho-ERK, phospho-p38, phospho-JNK, phospho-MAPKAPK (MK) 2, phospho-Syk, and total p38 were purchased from Cell Signaling Technology (Danvers, MA). The mouse mAb against total ERK2, APC-labeled anti-mouse CD11b mAb, APC- and PE-Cy5.5-labeled anti-mouse CD45.2 mAbs, the murine MCP-1 and MIP-1α ELISA kits were purchased from BD Biosciences (San Jose, CA). The rabbit polyclonal Abs against $gp91^{phox}$, $p47^{phox}$, $p67^{phox}$, JNK1 (C-17), Mkp-1 (V-15), and Mkp-1 (M-18) were purchased from Santa Cruz Biotechnology (Santa Cruz, CA). The mouse mAb against phosphotyrosine (4G10) and recombinant active p38 were purchased from Upstate Biotechnology (Lake Placid, NY). The mouse mAb against murine α-tublin and β-actin, luminol, isoluminol, 10-acetyl-3,7-dihydroxyphenoxazine (ADHP), hydrogen peroxide

(H_2O_2), and other common chemicals were purchased from Sigma Chemicals (St Louis, MO). The rabbit Ab against the murine Gsr was described previously (36). The rat CD16/CD32 mAb, mouse Syk mAb, Pacific blue- and Brilliant violet 421-labeled anti-mouse Ly6G mAbs, Brilliant violet 785-labeled anti-mouse Ly6C mAb, Pacific blue- and Alexa Fluor 488-labeled anti-mouse F4/80 mAbs were purchased from BioLegend (San Diego, CA). Enzyme-linked immunosorbent assay (ELISA) kits for murine TNF-α and IL-6 were purchased from eBiosciences (San Diego, CA). Murine IL-1β and KC ELISA kits were purchased from BioLegend and R&D Systems (Minneapolis, MN), respectively.

Mice

The *Gsr*$^{-/-}$ mice were generated after crossing the *Gsr* hypomorphic mice (36, 37) with C3H/HeN mice (Harlan Sprague Dawley, Indianapolis, IN) 10 generations (34, 35). WT C3H/HeN and *Gsr*$^{-/-}$ mice were kept at 25°C in a specific pathogen-free vivarium with a 12-h alternating light-dark cycle. Both male and female mice between 2 and 6 months of age were used in the study. All animal experiments were approved and conducted according to regulations of the Institutional Animal Care and Use Committee of the Research Institute at Nationwide Children's Hospital.

C. albicans infection, fungal burden determination, and pathology

C. albicans (SC5414) yeast was grown in YPD medium and *C. albicans* hyphae were made by additional culture in RPMI 1640 medium overnight (38). Mice were infected intravenously through the tail vein at a dose of 5×10^5 *C. albicans* yeast per mouse (39). To assess survival, these mice were monitored over 7 days. To assess blood cytokine levels, tissue and blood fungal burden, and organ pathology, mice were euthanized at specific time-points by ketamine/xylazine overdose to harvest blood and organs. Blood samples were serially diluted in PBS, and 10 μl of the diluted blood was spotted in quadruplicate on YPD plates. To determine fungal burden in organs, organs were excised aseptically, and homogenized in PBS in a Bullet blender at 4°C. The homogenates were serially diluted and spotted in quadruplicate on YPD plates. These plates were cultured at 30°C for 24–48 h to score for colony forming units.

To assess tissue pathology, tissues were fixed in formalin for 24–48 h, washed, and embedded in paraffin to prepare 4-μm sections. Adjacent sections were stained either with H&E or with periodic acid-Schiff (PAS) techniques, as previously described (38, 40).

Kidney MPO activity

Peroxidase activity in kidney homogenates was assessed as previously described (41). Briefly, 10 μl kidney homogenates (20 μg protein) were mixed with 39 μl PBS, 1 μl of 0.03% hydrogen peroxide (H_2O_2), and 50 μl of 200 μM ADHP solution. The assays were performed immediately at 37°C in a 96-well plate, and fluorescence readings were acquired with a SpectraMax® *M2* Multimode Microplate Readers (Molecular Device, Sunnyvale, CA), using excitation of 535 nm and emission of 590 nm for a total of 15 kinetic cycles with an interval of 20 s per cycle. Enzyme activities in the wells were defined as the slopes of the fluorescence vs. time curves.

Neutrophil isolation and macrophage derivation

Neutrophils were isolated by negative selection from bone marrow (BM) cells harvested from mouse femurs and tibias using a mouse neutrophil isolation kit (Miltenyl Biotec, Bergisch Gladbach, Germany). Cells were suspended in HBSS containing $CaCl_2$ and $MgCl_2$ (Invitrogen, Carlsbad, CA) supplemented with 0.5% BSA (Invitrogen) and 2% FBS (Hyclone, Logan, UT), and counted using a hemocytometer. The purity of neutrophils, evaluated by flow cytometry using Pacific blue-labeled anti-mouse Ly6G, consistently exceeded 90%.

BM cells were cultured on petri dishes in DMEM supplemented with 10% FBS, 25% L929-conditioned medium, and 40 ng/ml of recombinant mouse M-CSF (PeproTech, Rocky Hill, NJ). The cells were refed once with fresh medium after 4 days and cultured for 3 additional days to generate BM-derived macrophages (BMDM).

Leukocyte trafficking to kidneys

To investigate leukocyte trafficking to the kidneys, mice were euthanized by cervical dislocation 12 or 24 h post *C. albicans* infection. The mice were first perfused through the hearts with 10 ml cold PBS to clear blood from circulation. Kidneys were then excised and enzymatically digested in a solution containing 213 μg/ml Liberase (Roche Diagnostics, Mannheim, Germany), 100 μg/ml DNase I (Roche), and 40 μg/ml collagenase IV (Gibco, Gaithersburg, MD) at 37 °C for 20 min. The cell suspensions were then filtered through a 70-μm strainer, and pelleted by centrifugation, then resuspended in ACK buffer to lyse the red cells. Leukocytes were enriched through centrifugation using Percoll gradient. Leukocyte collected from the 40%–70% Percoll interface were then pelleted and suspended into 500 μl of FACS washing buffer (PBS containing 2.5% FBS). The cells were first blocked with 5 μg anti-CD16/CD32 mAb for 5 min, and then stained with 0.5 μg of APC-labeled anti-mouse CD11b mAb, 2 μg of PE-Cy5.5-labeled anti-mouse CD45.2 mAb, 1 μg of Brilliant violet 421-labeled anti-mouse Ly6G, 1 μg Brilliant violet 785-labeled anti-mouse Ly6C, and 2.5 μg Alexa Fluor 488-labeled anti-mouse F4/80 on ice for 10 min. Subsequently, the cells were washed twice with ice-cold FACS washing buffer prior to flow cytometry on a BD LSR II flow cytometer (BD Biosciences). Cells were gated based on the expression of leukocyte markers. $CD45^+CD11b^+Ly6G^+$ leukocytes were regarded as neutrophils, and $CD45^+CD11b^+Ly6C^{hi}$ were regarded as monocytes. $CD45^+CD11b^+F4/80^+$ leukocytes were regarded as macrophages. All flow cytometry data were analyzed using FlowJo software (FlowJo, Ashland, OR).

Neutrophil apoptosis was determined by flow cytometry after staining Percoll gradient-enriched leukocytes with 10 μg/ml anti-CD16/CD32 mAb, 4 μg/ml of APC-labeled anti-mouse CD45.2 mAb, 0.5 μg/ml of Brilliant violet 421-labeled anti-mouse Ly6G, as well as Alexa Flour 488-labeled annexin V and propidium iodide (PI) using an Alexa Fluor 488 Annexin V/Dead Cell Apoptosis kit (Invitrogen).

Respiratory burst assays

Neutrophil and macrophage respiratory burst *ex vivo* was assessed by bioluminescence in a 96-well format. Briefly, purified neutrophils were pre-incubated in 180 μl of HBSS

containing 0.5% BSA, 2% FBS, 100 μM luminol or isoluminol, 1.6 unit of horse radish peroxidase (EMD Biosciences, San Diego, CA) at room temperature for 10 min. Heat-killed, mouse serum-opsonized yeast (in 20 μl) were added into the wells to achieve a MOI of 10. PMA (dissolved in 20 μl reaction buffer) was directly added to the wells to achieve a concentration of 0.5 μM. Luminescence in each well was measured using a Synergy 2 luminometer (BioTek, Winooski, VT) for 1 s every 2 min consecutively for a given period. Cumulative respiratory burst activity was calculated as the integral of luminescence over a given time period. Respiratory burst in macrophages were measured similarly, with the following minor changes. BMDM were seeded at a density of 1×10^5 cells per well in 200 μl of complete medium on the day prior to the respiratory burst experiment. Before the respiratory burst experiment, 180 μl medium was removed from the wells, and replaced with HBSS containing 0.5% BSA, 2% FBS, 100 μM luminol or isoluminol, 1.6 unit of horse radish peroxidase. To assess intracellular oxidant production, 10 units of superoxide dismutase (Sigma Chemicals) and 400 units of catalase (Worthington Biochemical, Lakewood, NJ) were added in the luminol reactions, to eliminate the extracellular superoxide and hydrogen peroxide.

To assess oxidative burst activity *in vivo*, we carried out luminol bioluminescence imaging essentially as described by Gross et al. (42). Following *C. albicans* infection, each mouse was given one dose of luminol (200 μg/g b.w.) i.p. at a given time, and immediately placed in an IVIS Spectrum imaging system (PerkinElmer, Waltham, MA) to collect luminescent images (exposure time, 5 min; FOV, D; binning, 8).

Phagocytosis

Heat-killed *C. albicans* were labeled using a pHrodo™ Red Microscale Labeling Kit (Thermo Fisher Scientific, Waltham, MA), according to manufacturer's recommendation. Yeast cells were then washed three times with PBS and opsonized with 10% mouse serum at 37°C for 60 min. Neutrophils suspended in HBSS containing $CaCl_2$, $MgCl_2$, 0.5% BSA, and 2% FBS were incubated with pHrodo red-labeled, heat-killed, serum-opsonized yeast at a MOI of 3 or 10, either at 37°C or at 0°C for 30 min in a volume of 100 μl. Then, 1 μg of rat anti-mouse CD16/CD32 mAb and 0.5 μg of rat Pacific blue-conjugated anti-mouse Ly6G mAb were added into the neutrophil/yeast mixture to stain neutrophils on ice for 20 min. Subsequently, the cells centrifuged at 300×g for 5 min at 4°C, washed three time with 1 ml of ice-cold FACS washing buffer (PBS containing 0.5% BSA and 0.1% NaN_3), and finally suspended in ice-cold FACS washing buffer for flow cytometry.

To evaluate phagocytosis of *C. albicans* by macrophages, BMDM were plated onto 35-mm petri dishes in 2 ml DMEM containing 10% FBS at a density of 10^6 cells per plate. On the next day, pHrodo red-labeled heat-killed *C. albicans* were added into the medium at a MOI of 10. Then the plates were centrifuged at 300×g for 2 min at 37°C to sediment the yeast. After 30 min incubation at 37°C in 5% CO_2, the plates were washed twice with ice-cold PBS. Then 500 μl of PBS containing 0.5% BSA, 0.5 μg of Pacific blue-labeled anti-mouse F4/80 mAb, and 0.5 μg of anti-mouse CD16/CD32 mAb were added into the plates, and the plates were incubated on ice for 10 min. Subsequently, the plates were washed twice with ice-cold FACS washing buffer, and cells were collected by scrapping for flow cytometry.

Pacific blue-positive cells ($Ly6G^+$ neutrophils or $F4/80^+$ macrophages) that also displayed red fluorescence were regarded as neutrophils that engulfed *C. albicans*. All flow cytometry data were analyzed using FlowJo software (FlowJo, Ashland, OR).

C. albicans killing by neutrophils

Neutrophils isolated from BM were mixed with *C. albicans* yeast opsonized for 60 min with 10% normal mouse serum at a multiplicity of 10:1. Then the neutrophils/*C. albicans* mixtures were mixed with 10 volumes of sterile H_2O, serially diluted, and plated onto YPD agar plates. The plates were incubated at 37°C for approximately 24 h. Viable *C. albicans* cells were scored by counting the colonies formed on the YPD plates. The percent killing was calculated using the formula: % killing=(colony number of control - colony number of neutrophil-treated)/colony number of control×100.

Neutrophil subcellular fractionation

Neutrophils purified from mouse BM were stimulated with 0.5 μM PMA for 15 min or left unstimulated. Neutrophils were lysed, and the lysates were fractionated into membrane and cytosolic fractions by ultracentrifugation, as described (43).

Macrophage response to C. albicans stimulation

BMDM ($8–10\times10^6$ cells per plate) were seeded in 10 ml of DMEM (Invitrogen) containing 10% FBS and penicillin/streptomycin. To stimulate BMDM with *C. albicans*, heat-killed *C. albicans* were added into macrophage culture, and mixed thoroughly with medium. The plates were then centrifuged at 300×g for 2 min to sediment *C. albicans*. To harvest the cells, BMDM were washed twice with ice-cold PBS, and then lysed in 500 μl of lysis buffer, as previously described (44, 45). Cell lysates were centrifuged at 20,800×g for 10 min, and the supernatants were used for Western blot analysis.

To assess cytokine production, BMDM (5×10^5 cells per well) were seeded in 1 ml of complete medium on 12-well plates. On the next day, heat-killed *C. albicans* opsonized with mouse serum were added into the medium and mixed thoroughly. The plates were then centrifuged at 300×g for 2 min to sediment the yeast to the bottom of the wells. The cells were incubated at 37°C in humidified air containing 5% CO_2 for 24 or 48 h to harvest medium for ELISA.

TNF-α mRNA stability

BMDM were first stimulated with heat-killed *C. albicans* for 5.5 h, and then treated with either DMSO or SB203580 (final concentration, 10 μM) for an additional 30 min. Actinomycin D was added into the culture medium. Total RNA were harvested from the cells using Trizol (Invitrogen) after 0, 30, 60, and 90 min. TNF-α mRNA levels were quantified by qRT-PCR to assess TNF-α mRNA decay, as previously described (46, 47).

ELISA and Western blot analysis

ELISA and Western blot analyses were performed as previously described (40, 44, 48).

Mkp-1 activity assay

WT and *Gsr*$^{-/-}$ BMDM were stimulated with heat-killed *C. albicans* at an MOI of 5 for 4 h or left unstimulated. Soluble lysates (~900 μg protein) were precleaned with protein A-Sepharose beads (Amersham Pharmacia Biotech, Piscataway, NJ) at 4˚C for 30 min on a rotator, and then incubated with two rabbit polyclonal Abs against Mkp-1 (4 μg each, Mkp-1 (V15) and Mkp-1 (M18)) and protein A-Sepharose beads (25 μl) overnight at 4˚C on a rotator. Subsequently, the beads were washed twice with 1 ml lysis buffer and twice with lysis buffer supplemented with 150 mM NaCl. Recombinant active p38 (60 ng in 60 μl reaction buffer containing 50 mM Tris-HCl, pH7.4, 2 mM DTT, and 5 mM $MgCl_2$) was then incubated with the immunoprecipitates at 30˚C. A fraction (10 ng) of phospho-p38 was taken out at 0, 10, 30, and 90 min and mixed immediately with NuPAGE sample buffer containing 62.5 mM orthovanadate. The levels of phospho-p38 were assayed by Western blot analysis.

Statistics

The mortality data were compared using Kaplan-Meier's Log-Rank test. The values of various biomarkers were compared over time and between conditions using one-way ANOVA. Differences were identified using a modified t-test. *p* values of less than 0.05 were considered significant.

Results

Gsr$^{-/-}$ mice exhibit defective immune defense but elevated inflammatory response after C. albicans infection

To understand the tissue expression profile of Gsr, we isolated liver, lung, skeletal muscle, spleen, heart, kidney, brain, thymus, and eyes from WT and *Gsr*$^{-/-}$ mice. These organs were homogenized and tissue proteins were extracted. BM cells were flushed out from femurs and tibias and BM proteins were extracted. Western blot analyses were performed using a rabbit polyclonal Ab generated in house (SFig. 1). A clear band of ~53 kDa was detected in the liver, lung, spleen, kidney, brain, thymus, BM, and eyes of WT mice, but not in these tissues of *Gsr*$^{-/-}$ mice. A WT-specific band was not detected in skeletal muscle and heart tissues, suggesting that Gsr expression in muscle tissues was substantially lower than in other tissues. The relatively high expression of Gsr in BM, spleen, and thymus suggests that Gsr may play an important function in immune defense against pathogens.

To assess the role of Gsr in immune defense against fungal pathogens, we infected WT and *Gsr*$^{-/-}$ mice intravenously with live SC5414 *C. albicans*, and monitored the survival of these mice over 7 days (Fig. 1A). WT mice exhibited substantial resilience against *C. albicans*, with the first fatality occurring 4 days after *C. albicans* infection and 70% of the mice surviving after 7 days. In contrast to WT mice, *Gsr*$^{-/-}$ mice were considerably more sensitive to *C. albicans* infection. Substantial mortality was already observed one day after infection, and continued to increase rapidly. After 7 days, only 30% of the mice survived. The differences in survival rates ($p<0.05$) clearly illustrate the critical role of Gsr in host defense against fungal infections. In addition, the high mortality observed in *Gsr*$^{-/-}$ mice correlated with greater fungal burdens in the kidneys at 24 and 48 h after infection than in

WT mice (Fig. 1B). In keeping with this observation, severe inflammatory lesions associated with heavy *C. albicans* hyphae accumulation were observed in the kidneys of *C. albicans*-infected *Gsr*$^{-/-}$ mice but not in the kidneys of infected WT mice (Fig. 1C), as viewed by H&E and PAS staining, respectively. The fungal lesion in the kidneys of *C. albicans*-infected *Gsr*$^{-/-}$ mice contained almost entirely *C. albicans* hyphae (Fig. 1D). No *C. albicans* was detected in the blood or the spleens in either WT or *Gsr*$^{-/-}$ mice 24 or 48 h post inoculation (data not shown). Furthermore, inflammatory lesions were observed in the hearts of *C. albicans*-infected *Gsr*$^{-/-}$ mice but not in the hearts of WT mice (SFig. 2). Although inflammatory lesions with abundant neutrophils were frequently seen in the hearts of *C. albicans*-infected *Gsr*$^{-/-}$ mice, fungi were not detected in the hearts (data not shown). The presence of a larger number of neutrophils in the kidneys of *C. albicans*-infected *Gsr*$^{-/-}$ mice was also consistent with the greater *in vitro* MPO activity in the kidney homogenates of infected *Gsr*$^{-/-}$ mice than in those of the infected WT mice (Fig. 1E).

Leukocyte recruitment plays a crucial role in immune response, and defects in the trafficking of leukocytes, particularly phagocytes, could compromise immune defense and lead to organ dysfunction of the host (8, 49, 50). To examine whether *Gsr*$^{-/-}$ mice have defects in leukocyte trafficking during *C. albicans* infection, we assessed the cell numbers of neutrophils, macrophages, monocytes in the kidneys shortly (12 or 24 h) after *C. albicans* infection (Fig. 2A). Leukocytes were enriched by Percoll gradient centrifugation from enzymatically digested kidneys, and the numbers of neutrophils, macrophages, and monocytes were determined by flow cytometry. At 12 h post *C. albocans* infection, the number of neutrophils in the kidneys of *Gsr*$^{+/+}$ and *Gsr*$^{-/-}$ mice were similar. By 24 h, substantially more neutrophils were seen in the kidneys of *Gsr*$^{-/-}$ mice than in those of *Gsr*$^{+/+}$ mice. In fact, fewer neutrophils were seen in the kidneys of *Gsr*$^{+/+}$ mice at 24 h than at 12 h. While both macrophages and monocytes were seen in *Gsr*$^{-/-}$ mice, their numbers did not differ significantly between *Gsr*$^{+/+}$ and *Gsr*$^{-/-}$ mice at either 12 or 24 h time-point. Since neutrophils are the most potent leukocytes mediating *C. albicans* killing (8, 51), we assessed whether there were differences in the viabilities of the neutrophils in the kidneys between *Gsr*$^{+/+}$ and *Gsr*$^{-/-}$ mice (Fig. 2B). Necrotic and apoptotic neutrophils were assessed based on the staining by PI and annexin V. No differences were seen in the portions of necrotic, early or later apoptotic neutrophils between *C. albicans*-infected *Gsr*$^{+/+}$ and *Gsr*$^{-/-}$ mice. Thus, despite increased numbers of neutrophils in the kidneys of *Gsr*$^{-/-}$ mice, counter-intuitively these mice exhibited substantially elevated fungal burden and increased mortality, strongly supporting a defective fungicidal response in *Gsr*$^{-/-}$ mice.

Since inflammatory cytokines, particularly TNF-α, play a crucial role in the orchestration of the anti-fungal immune defense (52–54), we assessed the production of inflammatory cytokines in WT and *Gsr*$^{-/-}$ mice. Blood was harvested at different times following infection, and cytokine levels in the blood were measured by ELISA (Fig. 3). The levels of TNF-α, IL-6, MCP-1, and MIP-1α were comparable in WT and *Gsr*$^{-/-}$ mice at 6 h post-infection. Clear differences in the blood levels of IL-6 and MCP-1 between WT and *Gsr*$^{-/-}$ mice were seen at 24 h post-infection. By 48 h, the levels of all five serum cytokines (TNF-α, IL-6, MCP-1, MIP-1α, and KC) were substantially higher in *Gsr*$^{-/-}$ mice than in WT mice. These results clearly indicate that *Gsr*$^{-/-}$ mice can mount an inflammatory response as the result of *C. albicans* infection.

Compromised fungicidal activity of Gsr-deficient neutrophils

Respiratory burst in phagocytes play a pivotal role in the containment and killing of fungal pathogens (55, 56). We assess the respiratory burst activity *in vivo* following *C. albicans* infection, by luminol bioluminescence (42). In un-infected (control) mice, respiratory burst activity was undetectable in either $Gsr^{+/+}$ or $Gsr^{-/-}$ mice (Fig. 4, Upper panel). Respiratory burst activity was elevated in the abdominal region of $Gsr^{+/+}$ mice 12 h after *C. albicans* infection (Fig. 4, Mid panel) and plummeted to undetectable levels by 24 h (Fig. 4, Lower panel). No respiratory activity was detected at either 12 or 24 h in *C. albicans*-infected $Gsr^{-/-}$ mice (Fig 4).

To understand the basis underlying the immunological defect of $Gsr^{-/-}$ mice against *C. albicans*, we assessed the phagocytic activities of neutrophils purified from WT and $Gsr^{-/-}$ mice. Phagocytosis of *C. albicans* by $Ly6G^+$ neutrophils was assessed by flow cytometry (Fig. 5A). The percentage of WT $Ly6G^+$ neutrophils that engulfed *C. albicans* was 99.2%, while the percentage of $Gsr^{-/-}$ neutrophils that engulfed *C. albicans* was 95.5%. Although the percentage of neutrophils that engulfed *C. albicans* did not markedly differ between WT and $Gsr^{-/-}$ groups, WT neutrophils engulfed substantially more *C. albicans* than did $Gsr^{-/-}$ neutrophils on a per cell basis, indicated by greater mean fluorescent intensity (12,036 vs 5,204 arbitrary units/cell for WT and $Gsr^{-/-}$ cells, respectively). The results suggest that Gsr is required for effective phagocytosis of *C. albicans* in neutrophils.

To assess whether $Gsr^{-/-}$ neutrophils exhibit a decline in fungicidal activity, *in vitro* fungicidal assays were performed. Live *C. albicans* yeast were incubated with WT and $Gsr^{-/-}$ neutrophils at a MOI of 10 for 60 min, and then neutrophils were lysed by hypo-osmolarity. The surviving *C. albicans* yeast were cultured on YPD plates and quantified. Compared with WT neutrophils that killed 33% of *C. albicans* yeast, $Gsr^{-/-}$ neutrophils killed only 17% of *C. albicans* yeast, clearly indicating a defect in fungicidal activity (Fig. 5B).

Since the NADPH oxidase-mediated respiratory burst is a major microbicidal mechanism of neutrophils (21, 56) and a diminished respiratory burst activity was seen in *C. albicans*-infected $Gsr^{-/-}$ mice *in vivo* (Fig. 6), we assessed respiratory burst activity in WT and $Gsr^{-/-}$ neutrophils. Respiratory burst was measured by chemiluminescence *in vitro*. The kinetics of total ROS production in WT and $Gsr^{-/-}$ neutrophils assessed using luminol after stimulation with *C. albicans* are depicted in Figure 6A (*Upper graph*). Intracellular ROS was measured in the presence of SOD and catalase in order to eliminate extracellular ROS (Fig. 6A, *Middle graph*). Extracellular ROS was detected using isoluminol (Fig. 6A, *Lower graph*), as the cell membrane is impermeable to isoluminol. In WT neutrophils, both extracellular and intracellular production of ROS increased with *C. albicans* stimulation and reached peak levels at about 5–6 h, followed by a decline. ROS production was also enhanced by *C. albicans* stimulation in $Gsr^{-/-}$ neutrophils, but did not reach the levels of WT neutrophils. The cumulative production of ROS both intracellularly and extracellularly in $Gsr^{-/-}$ neutrophils following *C. albicans* stimulation were significantly lower than those in WT neutrophils (Fig. 6B). Similarly, lower ROS production was also observed in $Gsr^{-/-}$ neutrophils following PMA stimulation (Fig. 6B).

Previously, it has been shown that vitamin E pre-treatment of neutrophils isolated from GSR-deficient human subjects rescued their pentose phosphatase shunt activity (33), a metabolic reaction responsible for the generation of NADPH, a substrate for neutrophil respiratory burst. We assessed whether vitamin E alleviates the respiratory burst defects of *Gsr*$^{-/-}$ neutrophils (Fig. 6C). Neutrophils were preincubated with vitamin E for 30 min prior to the initiation of respiratory burst by PMA. While vitamin E enhanced the respiratory burst by sustaining the maximal respiratory burst activity in WT neutrophils, vitamin E did not markedly change the kinetics of PMA-triggered respiratory burst in *Gsr*$^{-/-}$ neutrophils (Fig. 6C).

To understand the mechanism underlying the respiratory burst defect in *Gsr*$^{-/-}$ neutrophils, we studied the membrane assembly of NADPH oxidase subunits and signal transduction pathways known to regulate NADPH oxidase activation. WT and *Gsr*$^{-/-}$ neutrophils purified from BM were stimulated with or without PMA, lyzed, and fractionated by centrifugation into cytosolic and membrane fractions. Different NADPH subunits were detected by Western blot analysis (Fig. 7A). Consistent with previous reports that gp91^{phox} localizes in the membrane as a glycosylated protein (57, 58), gp91^{phox} was detected in the membrane fraction in both WT and *Gsr*$^{-/-}$ neutrophils. In response to PMA stimulation, the abundance of membrane-associated gp91^{phox} actually decreased in both groups. In contrast, both p67^{phox} and p47^{phox} subunits were predominantly localized in the cytosolic fractions. However, in response to PMA stimulation, a small fraction of both p47^{phox} and p67^{phox} were translocated into the membrane fractions. No differences were found between WT and *Gsr*$^{-/-}$ neutrophils in the localization of these subunits, suggesting that Gsr deficiency does not affect the assembly of the NADPH oxidase complexes.

A number of protein kinases, including ERK and p38 MAPKs as well as Syk tyrosine kinase have been shown to regulate neutrophil respiratory burst (22, 24, 59). To assess whether alterations in these kinases could contribute to the defective respiratory burst of *Gsr*$^{-/-}$ neutrophils, we assayed the activities of ERK and p38 and examined global tyrosine phosphorylation in stimulated neutrophils (Figs. 7B & C). Interestingly, PMA-induced ERK activity was substantially stronger in *Gsr*$^{-/-}$ neutrophils than in similarly treated WT neutrophils, although PMA-stimulated p38 activity was similar in the two groups (Fig. 7B). *C. albicans*-induced ERK activity was also slightly stronger in *Gsr*$^{-/-}$ neutrophils than in WT neutrophils (Fig. 7C, Upper panel). Furthermore, PMA-induced tyrosine phosphorylation was dramatically stronger in *Gsr*$^{-/-}$ neutrophils than in WT neutrophils (Fig. 7C, Lower panel). These tyrosine-phosphorylated proteins triggered by PMA covered a wide range of molecular masses, from ~20 –200 kDa. *C. albicans* also triggered the tyrosine phosphorylation of several proteins in the 30–65 kDa range in *Gsr*$^{-/-}$ neutrophils (marked with asterisks in Fig. 7C), but not in WT neutrophils.

Enhanced inflammatory activity of Gsr$^{-/-}$ macrophages

To understand whether macrophages in *Gsr*$^{-/-}$ mice contribute to the abnormality in the immune defense against *C. albicans*, BMDM were stimulated with different doses of heat-killed *C. albicans*. *C. albicans* were heat-killed to avoid the complication of varying stimuli due to potential differences in the killing of *C. albicans* between WT and *Gsr*$^{-/-}$

macrophages. The medium was harvested after 24 or 48 h, and assayed for cytokine production. TNF-α production was dramatically increased following *C. albicans* stimulation in both groups. Significantly more TNF-α was produced by *Gsr*$^{-/-}$ macrophages than by WT macrophages (Fig. 8A). More IL-6 and IL-1β were also produced by *Gsr*$^{-/-}$ macrophages than by WT cells following *C. albicans* stimulation. The enhanced cytokine production in *Gsr*$^{-/-}$ macrophages was not caused by differences in phagocytic activity between WT and *Gsr*$^{-/-}$ macrophages, since the phagocytic activity of the two groups were similar (Fig. 8B). These results clearly indicate that *Gsr*$^{-/-}$ macrophages are functionally competent in the detection of *C. albicans*.

Since MAPKs, particularly ERK, have been shown to regulate the production of inflammatory cytokines following *C. albicans* stimulation (60–62), we assessed whether Gsr deficiency alters MAPK activities (Fig. 9A). Upon stimulation with heat-killed *C. albicans*, ERK activity was rapidly increased in both WT and *Gsr*$^{-/-}$ macrophages, and reached peak levels at ~15 min. Although the peak levels of ERK activity, indicated by the density of the phospho-ERK bands, were not different between WT and *Gsr*$^{-/-}$ macrophages, ERK activity was slightly higher at the later time points (2 and 4 h) in *Gsr*$^{-/-}$ macrophages. *C. albicans* stimulation also triggered a rapid increase in the activities of JNK and p38 within 15 min in both WT and *Gsr*$^{-/-}$ macrophages. However, JNK activity rebounded by 4 h in *Gsr*$^{-/-}$ macrophages but not in WT macrophages. In WT macrophages, p38 activity declined after the peak and then modestly rebounded between 2 and 4 h. In contrast, p38 activity slightly decreased at 45 min and then increased dramatically between 2 to 4 h in *Gsr*$^{-/-}$ macrophages. Substantially elevated MK2 activity (63), which is regulated by p38 (64), was seen in *C. albicans*-stimulated *Gsr*$^{-/-}$ macrophages but not in WT macrophages.

In macrophages, the activity of JNK and p38 are negatively regulated by Mkp-1, a dual specificity protein phosphatase (40, 44, 48, 65), and attenuated Mkp-1 activity could enhance both JNK and p38 activities. To measure the activity of Mkp-1, we immunoprecipitated Mkp-1 from unstimulated and *C. albicans*-stimulated macrophages, and assessed the enzymatic activity of Mkp-1 *in vitro* using recombinant active p38 as a substrate (Fig. 9B). Incubation of active p38 with immunoprecipitated Mkp-1 resulted in a time-dependent decline in p38 phosphorylation, detected by Western blotting (Fig. 9B). Compared to Mkp-1 immunoprecipitated from WT macrophages, the activity of Mkp-1 immunoprecipitated from *Gsr*$^{-/-}$ macrophages was lower than that of WT macrophages, indicated by the greater phospho-p38 levels at the corresponding time-points.

Since p38 has been shown to regulate the stability of the mRNAs containing AU-rich elements in their 3' untranslated regions of a variety of cytokines, including TNF-α (66), we assessed the stability of TNF-α mRNA in *C. albicans*-stimulated *Gsr*$^{+/+}$ and *Gsr*$^{-/-}$ macrophages (Fig. 9C). While the half-life of TNF-α mRNA in *C. albicans*-treated *Gsr*$^{+/+}$ macrophages was 24 min, the half-life was increased to 49 min in similarly treated *Gsr*$^{-/-}$ macrophages (Fig. 9C). The p38 inhibitor, SB203580, almost completely abrogated the increase in the stability of TNF-α mRNA in *Gsr*$^{-/-}$ macrophages.

Syk plays a critical role in the orchestration of the signal transduction pathways in response to *C. albicans* stimulation (11–13). Syk activation is associated with autophosphorylation at

the Tyr525/526 site (67). We assessed whether *C. albicans*-stimulated Syk phosphorylation at the Tyr525/526 site in *Gsr*$^{-/-}$ macrophages is different from that in WT cells (Fig. 9D). *C. albicans* hypha stimulation only slightly increased Syk phosphorylation at the Tyr525/526 site in WT macrophages. In contrast, Syk phosphorylation at the Tyr525/526 site was markedly increased in *Gsr*$^{-/-}$ macrophages after exposure to *C. albicans* hyphae, although the total Syk levels were similar to those in WT macrophages. Syk phosphorylation at Tyr525/526 was detectable within 15 min following *C. albicans* stimulation and lasted for at least 4 h. The levels of tyrosine phosphorylation in multiple proteins were dramatically increased in *C. albicans* hypha-stimulated *Gsr*$^{-/-}$ macrophages but not in WT macrophages. Taken together, these results strongly support an unexpected role of Gsr in the restraint of the inflammatory response of macrophages following *C. albicans* infection through the negative regulation of the Syk tyrosine kinase cascade.

Discussion

Gsr$^{-/-}$ mice were found to be highly susceptible to *C. albicans*. In the absence of *Gsr*, *C. albicans* infection caused a markedly elevated fungal burden (Fig. 1B), blood cytokine storm (Fig. 3), and substantially increased mortality (Fig. 1A). Since large numbers of inflammatory leukocytes, including neutrophils, were found in the proximity of the fungal lesions in the kidneys of *Gsr*$^{-/-}$ mice (Figs. 1C & D), Gsr deficiency did not appear to hinder the leukocyte trafficking to the kidneys. The higher kidney fungal burdens in *Gsr*$^{-/-}$ mice (Figs. 1B & C) in spite of the greater numbers of neutrophils in the kidneys (Figs. 1C, 1E, and 2A) clearly indicate a profound defect in the fungicidal mechanisms in these mice. In support of this notion, we observed a marked decline in the phagocytosis activity and a significant impairment in fungicidal activity in *Gsr*$^{-/-}$ neutrophils (Fig. 5). The decreased respiratory burst activity of *Gsr*$^{-/-}$ neutrophils (Fig. 6) provides a mechanistic explanation for the markedly diminished respiratory burst activity *in vivo* (Fig. 4) and compromised immune defense against *C. albicans* in *Gsr*$^{-/-}$ mice. *Gsr*$^{-/-}$ neutrophils appeared to undergo normal NAPDH oxidase assembly on the membrane and was associated with profound enhancements of overall tyrosine phosphorylation and ERK activation (Fig. 7). We found that Gsr also plays a significant role in macrophages. In response to heat-killed *C. albicans,* *Gsr*$^{-/-}$ macrophages exhibited elevated Syk, p38 and JNK activities (Fig. 9), and produced increased inflammatory cytokines TNF-α, IL-1β, and IL-6 (Fig. 8A), although Gsr deficiency in macrophages had little impact on *C. albicans* uptake (Fig. 8B). Our studies demonstrate that although *Gsr*$^{-/-}$ mice are competent in detecting *C. albicans* pathogens and mobilizing inflammatory leukocytes to the infection site, their neutrophils are impaired in capturing and killing of these pathogens. Our studies revealed critical functions of Gsr in both neutrophils and macrophages, two key cell types of the innate immune defense.

The function of Gsr in neutrophils

While exactly how Gsr facilitates neutrophil-mediated *C. albicans* killing is not completely understood, few possible mechanisms could be considered. First, it is possible that Gsr protects the fungicidal machinery of neutrophils by maintaining the level of GSH. Upon encountering fungi or yeast, neutrophils produce large amounts of ROS in the phagolysosomes, which are crucial for the killing of the pathogens (21, 68). However,

phagolysosomal ROS, H_2O_2 in particular, could also leak into the cytosol, leading to harmful oxidation of cellular components. In the cytosol, GSH can detoxify H_2O_2 and becomes GSSG. Because Gsr catalyzes the regeneration of GSH from GSSG, it is conceivable that WT neutrophils would be able to maintain a significant level of GSH in the cytosol to detoxify cytosolic ROS and thereby protect the cells. In contrast, GSH cannot be regenerated in *Gsr*$^{-/-}$ neutrophils and upon depletion of GSH, ROS leaked out from the phagolysosomes will remain unopposed in reacting with the cellular organelles and enzymes, including those responsible for the generation of NADPH from glucose. The notable increase in global protein tyrosine phosphorylation in *Gsr*$^{-/-}$ neutrophils following PMA stimulation is also consistent with the exposure to elevated oxidants; H_2O_2 is known to inhibit tyrosine phosphatases, thereby leading to global protein tyrosine phosphorylation (69–71). Such oxidative damage could impair the phagocytosis of *C. albicans*, halt the pentose monophosphate pathway, and terminate NADPH oxidase-mediated respiratory burst. It is worth noting that the cessation of the respiratory burst in *Gsr*$^{-/-}$ neutrophils following PMA stimulation was not caused by death of these cells, as the vast majority of the neutrophils were not stained by PI (data not shown).

A second but related possibility is that the compromised respiratory burst in *Gsr*$^{-/-}$ neutrophils may be the result of a dramatic signaling disarray. In *Gsr*$^{-/-}$ neutrophils, PMA stimulation resulted in a profound increase in both global protein tyrosine phosphorylation and ERK activation (Fig. 7C). We speculate that the substantially elevated global tyrosine phosphorylation may only represent the '*tip of the iceberg*' in a dramatic signaling disarray, as other biological processes could also be affected but not easily detectable. Nonetheless, it is conceivable that the aberrant signaling disarray ultimately leads to the termination of the intricately organized respiratory burst process. Neutrophil signaling disarray or enzymatic inhibition in *Gsr*$^{-/-}$ neutrophils during the phagocytosis may also explain why fewer yeast particles are engulfed and killed by *Gsr*$^{-/-}$ neutrophils than by WT cells (Fig. 5), since respiratory burst occurs simultaneously as cells engulf yeast particles (72). While ERK has been shown to regulate the respiratory burst through phosphorylation of p47^{phox} (22, 24, 59), the elevated ERK activity in *Gsr*$^{-/-}$ neutrophils (Figs. 7B & C) cannot explain the decline in respiratory burst activity in these cells. Since ERK activation in response to PMA is mediated by PKCs, a kinase family critical for neutrophil respiratory burst (22), based on the greater ERK activity we reason that a defect in PKC activation in *Gsr*$^{-/-}$ neutrophils is unlikely. A third possibility is that Gsr may facilitate the assembly or modification of the NADPH oxidase subunits, although we think that this is unlikely. In PMA-stimulated neutrophils, both p67^{phox} and p47^{phox} subunits of the NADPH oxidase complex were recruited to the membrane and the membrane-associated gp91^{phox} subunit underwent similar changes in both WT and *Gsr*$^{-/-}$ cells after PMA stimulation (Fig. 7A). These results combined with the normal initial respiratory burst in the first few minutes following PMA stimulation in *Gsr*$^{-/-}$ neutrophils (33, 34) strongly suggest that NADPH oxidase assembly, at least in the early phase, is not affected by Gsr deficiency.

The function of Gsr in macrophages

Another interesting finding of this study is that *Gsr*$^{-/-}$ mice and macrophages produce higher amounts of cytokines and chemokines than do their WT counterparts (Figs. 3 & 8).

While increased fungal burden may contribute to the elevated cytokines and chemokines in *C. albicans*-challenged *Gsr*$^{-/-}$ mice, *Gsr*$^{-/-}$ macrophages also appeared to exhibit enhanced intrinsic inflammatory responses following fungal stimulation. This is reflected in the elevated cytokine production *in vitro* following stimulation with heat-killed *C. albicans* (Fig. 8) and greater levels of p38 and JNK activities (Fig. 9A). Given that *C. albicans* used in these experiments were heat-killed and both WT and *Gsr*$^{-/-}$ macrophages engulfed similar amounts of *C. albicans* (Fig. 8B), the increased cytokine production and elevated p38 and Syk activities strongly suggest a greater sensitivity of *Gsr*$^{-/-}$ cells to *C. albicans* stimulation. We think that two mechanisms could contribute to the enhanced cytokine production in *Gsr*$^{-/-}$ macrophages. First, the increased Syk activity and enhanced global tyrosine phosphorylation may enhance the inflammatory response to yeast through augmenting the ERK pathway (Fig. 9A, D). Second, p38 may contribute to the inflammatory response by enhancing the stabilities and the translation of the AU-rich element-containing cytokine mRNAs. TNF-α mRNA was substantially more stable in *Gsr*$^{-/-}$ macrophages than in the wildtype macrophages, and TNF-α mRNA stabilization caused by Gsr deficiency was almost completely abolished by the p38 inhibitor (Fig. 9C), highlighting the critical role of enhanced p38 activation in the augmented inflammatory response. Enhanced mRNA stability may also contribute to the increased production of other cytokines, such as IL-6 and IL-1β (Fig. 8).

While it is not entirely unclear how Gsr deficiency causes enhanced Syk and MAPK activation, based on the biochemical function of Gsr we can make some speculation. Many protein kinases, particularly tyrosine kinases and MAPKs whose activation requires tyrosine phosphorylation, are negatively regulated by protein tyrosine phosphatases (73). Protein tyrosine phosphatases rely on a cysteine residue in the catalytic site, (H/V)CX_5R(S/T), for tyrosine dephosphorylation. The MAPK phosphatases have a similar catalytic site (VHCX5R(S/T)) (74, 75), with cysteine being essential for MAPK dephosphorylation. If the thiol residue in their catalytic sites is oxidized by ROS, these phosphatases become functionally inactive. GSH may play a crucial role in the protection of these cysteine residues in tyrosine phosphatases and dual specificity phosphatases including Mkp-1. In the absence of Gsr, GSSG cannot be regenerated into GSH. Once GSH is depleted by cytosolic ROS as the result of respiratory burst, cytosolic proteins such as protein tyrosine phosphatases and Mkps will become vulnerable to oxidation, leading to exuberant tyrosine kinase and MAPK activation. This model is consistent with the observation that Mkp-1 activity in *Gsr*$^{-/-}$ macrophages is lower than that of wildtype macrophages (Fig. 9B). This model also explains why sustained Syk, JNK, and p38 activation and global tyrosine phosphorylation only occurs hour(s) after *C. albicans* stimulation, because GSH depletion only occurs after a period of respiratory burst. The respiratory burst in neutrophils induced by PMA is substantially more robust than that induced by yeast in neutrophils (Fig. 6B) or macrophages (76). Therefore, it is not surprising that dramatically greater global tyrosine phosphorylation is seen in PMA-stimulated *Gsr*$^{-/-}$ neutrophils than in yeast- or PMA-treated macrophages (Fig. 7C & 9C). The difference in the amounts of ROS produced by neutrophils and macrophages may also explain why Gsr deficiency preferentially compromises the phagocytosis of neutrophils (Fig. 5A) but not macrophages (Fig. 8B). Because neutrophils produce far more ROS than the macrophages (76), Gsr deficiency is

expected to result in greater oxidative damage and have a larger impact on phagocytosis in neutrophils than in macrophages.

Supplementary Material

Refer to Web version on PubMed Central for supplementary material.

Acknowledgments

We want to thank Sara A. Crowell for technical support. We are also grateful to Dr. Victoria Best and Dave Dunaway for assistance in flow cytometry.

The studies were supported by NIH grants (AI113930 and AI124029 to Y.L., and AI121196 and AI123253 to J.Z.).

References

1. Hidron AI, Edwards JR, Patel J, Horan TC, Sievert DM, Pollock DA, and Fridkin SK 2008 NHSN annual update: antimicrobial-resistant pathogens associated with healthcare-associated infections: annual summary of data reported to the National Healthcare Safety Network at the Centers for Disease Control and Prevention, 2006–2007. Infect. Control Hosp. Epidemiol. 29: 996–1011. [PubMed: 18947320]
2. Richards MJ, Edwards JR, Culver DH, and Gaynes RP 1999 Nosocomial infections in medical intensive care units in the United States. National Nosocomial Infections Surveillance System. Crit Care Med. 27: 887–892. [PubMed: 10362409]
3. CDC. 2013 Antibiotic resistance threats in the United States, 2013: Flucozazole-resistant Candida.
4. Wisplinghoff H, Ebbers J, Geurtz L, Stefanik D, Major Y, Edmond MB, Wenzel RP, and Seifert H 2014 Nosocomial bloodstream infections due to Candida spp. in the USA: species distribution, clinical features and antifungal susceptibilities. Int. J. Antimicrob. Agents 43: 78–81. [PubMed: 24182454]
5. Magill SS, Edwards JR, Bamberg W, Beldavs ZG, Dumyati G, Kainer MA, Lynfield R, Maloney M, McAllister-Hollod L, Nadle J, Ray SM, Thompson DL, Wilson LE, and Fridkin SK 2014 Multistate point-prevalence survey of health care-associated infections. N. Engl. J. Med 370: 1198–1208. [PubMed: 24670166]
6. Pfaller MA, and Diekema DJ 2007 Epidemiology of invasive candidiasis: a persistent public health problem. Clin. Microbiol. Rev 20: 133–163. [PubMed: 17223626]
7. Kett DH, Azoulay E, Echeverria PM, and Vincent JL 2011 Candida bloodstream infections in intensive care units: analysis of the extended prevalence of infection in intensive care unit study. Crit Care Med 39: 665–670. [PubMed: 21169817]
8. Netea MG, Joosten LA, van der Meer JW, Kullberg BJ, and van de Veerdonk FL 2015 Immune defence against Candida fungal infections. Nat. Rev. Immunol 15: 630–642. [PubMed: 26388329]
9. Dambuza IM, and Brown GD 2015 C-type lectins in immunity: recent developments. Curr. Opin. Immunol 32:21–7. doi: 10.1016/j.coi.2014.12.002. Epub;%2014 Dec 29.: 21–27. [PubMed: 25553393]
10. Goodridge HS, Wolf AJ, and Underhill DM 2009 Beta-glucan recognition by the innate immune system. Immunol. Rev 230: 38–50. [PubMed: 19594628]
11. Reid DM, Gow NA, and Brown GD 2009 Pattern recognition: recent insights from Dectin-1. Curr. Opin. Immunol 21: 30–37. [PubMed: 19223162]
12. Kerrigan AM, and Brown GD 2011 Syk-coupled C-type lectins in immunity. Trends Immunol. 32: 151–156. [PubMed: 21334257]
13. Kerrigan AM, and Brown GD 2010 Syk-coupled C-type lectin receptors that mediate cellular activation via single tyrosine based activation motifs. Immunol. Rev 234: 335–352. [PubMed: 20193029]
14. Netea MG, and Marodi L 2010 Innate immune mechanisms for recognition and uptake of Candida species. Trends Immunol. 31: 346–353. [PubMed: 20705510]

15. Zhu LL, Zhao XQ, Jiang C, You Y, Chen XP, Jiang YY, Jia XM, and Lin X 2013 C-type lectin receptors Dectin-3 and Dectin-2 form a heterodimeric pattern-recognition receptor for host defense against fungal infection. Immunity. 39: 324–334. [PubMed: 23911656]
16. Zhu LL, Luo TM, Xu X, Guo YH, Zhao XQ, Wang TT, Tang B, Jiang YY, Xu JF, Lin X, and Jia XM 2016 E3 ubiquitin ligase Cbl-b negatively regulates C-type lectin receptor-mediated antifungal innate immunity. J. Exp. Med 213: 1555–1570. [PubMed: 27432944]
17. Saijo S, and Iwakura Y 2011 Dectin-1 and Dectin-2 in innate immunity against fungi. Int. Immunol 23: 467–472. [PubMed: 21677049]
18. Marino MW, Dunn A, Grail D, Inglese M, Noguchi Y, Richards E, Jungbluth A, Wada H, Moore M, Williamson B, Basu S, and Old LJ 1997 Characterization of tumor necrosis factor-deficient mice. Proc. Natl. Acad. Sci. U. S. A 94: 8093–8098. [PubMed: 9223320]
19. Conti HR, and Gaffen SL 2015 IL-17-Mediated Immunity to the Opportunistic Fungal Pathogen Candida albicans. J. Immunol 195: 780–788. [PubMed: 26188072]
20. Gaffen SL, Hernandez-Santos N, and Peterson AC 2011 IL-17 signaling in host defense against Candida albicans. Immunol. Res 50: 181–187. [PubMed: 21717069]
21. Klebanoff SJ, and Clark RA 1978 The neutrophil: Function and clinical disorders. North-Holland Publishing Company, Amsterdam.
22. Lambeth JD 2004 NOX enzymes and the biology of reactive oxygen. Nat. Rev. Immunol 4: 181–189. [PubMed: 15039755]
23. Babior BM 2004 NADPH oxidase. Curr. Opin. Immunol 16: 42–47. [PubMed: 14734109]
24. Van Ziffle JA, and Lowell CA 2009 Neutrophil-specific deletion of Syk kinase results in reduced host defense to bacterial infection. Blood 114: 4871–4882. [PubMed: 19797524]
25. Cheng N, He R, Tian J, Dinauer MC, and Ye RD 2007 A critical role of protein kinase C delta activation loop phosphorylation in formyl-methionyl-leucyl-phenylalanine-induced phosphorylation of p47(phox) and rapid activation of nicotinamide adenine dinucleotide phosphate oxidase. J. Immunol 179: 7720–7728. [PubMed: 18025218]
26. Inanami O, Johnson JL, McAdara JK, Benna JE, Faust LR, Newburger PE, and Babior BM 1998 Activation of the leukocyte NADPH oxidase by phorbol ester requires the phosphorylation of p47PHOX on serine 303 or 304. J. Biol. Chem 273: 9539–9543. [PubMed: 9545283]
27. El BJ, Han J, Park JW, Schmid E, Ulevitch RJ, and Babior BM 1996 Activation of p38 in stimulated human neutrophils: phosphorylation of the oxidase component p47phox by p38 and ERK but not by JNK. Arch. Biochem. Biophys 334: 395–400. [PubMed: 8900416]
28. Heyworth PG, Cross AR, and Curnutte JT 2003 Chronic granulomatous disease. Curr. Opin. Immunol 15: 578–584. [PubMed: 14499268]
29. Reed PW 1969 Glutathione and the hexose monophosphate shunt in phagocytizing and hydrogen peroxide-treated rat leukocytes. J. Biol. Chem 244: 2459–2464. [PubMed: 5783842]
30. Strauss RR, Paul BB, Jacobs AA, and Sbarra AJ 1969 The role of the phagocyte in host-parasite interactions. XIX. Leukocytic glutathione reductase and its involvement in phagocytosis. Arch. Biochem. Biophys 135: 265–271. [PubMed: 4391340]
31. Cohen HJ, Tape EH, Novak J, Chovaniec ME, Liegey P, and Whitin JC 1987 The role of glutathione reductase in maintaining human granulocyte function and sensitivity to exogenous H2O2. Blood 69: 493–500. [PubMed: 3801665]
32. Loos H, Roos D, Weening R, and Houwerzijl J 1976 Familial deficiency of glutathione reductase in human blood cells. Blood 48: 53–62. [PubMed: 947404]
33. Roos D, Weening RS, Voetman AA, van Schaik ML, Bot AA, Meerhof LJ, and Loos JA 1979 Protection of phagocytic leukocytes by endogenous glutathione: studies in a family with glutathione reductase deficiency. Blood 53: 851–866. [PubMed: 435643]
34. Yan J, Meng X, Wancket LM, Lintner K, Nelin LD, Chen B, Francis KP, Smith CV, Rogers LK, and Liu Y 2012 Glutathione reductase facilitates host defense by sustaining phagocytic oxidative burst and promoting the development of neutrophil extracellular traps. J. Immunol 188: 2316–2327. [PubMed: 22279102]
35. Yan J, Ralston MM, Meng X, Bongiovanni KD, Jones AL, Benndorf R, Nelin LD, Joshua FW, Rogers LK, Smith CV, and Liu Y 2013 Glutathione reductase is essential for host defense against bacterial infection. Free Radic. Biol. Med 61C: 320–332.

36. Rogers LK, Tamura T, Rogers BJ, Welty SE, Hansen TN, and Smith CV 2004 Analyses of glutathione reductase hypomorphic mice indicate a genetic knockout. Toxicol. Sci 82: 367–373. [PubMed: 15342956]
37. Pretsch W 1999 Glutathione reductase activity deficiency in homozygous Gr1a1Neu mice does not cause haemolytic anaemia. Genet. Res 73: 1–5. [PubMed: 10218442]
38. Xiao Y, Tang J, Guo H, Zhao Y, Tang R, Ouyang S, Zeng Q, Rappleye CA, Rajaram MV, Schlesinger LS, Tao L, Brown GD, Langdon WY, Li BT, and Zhang J 2016 Targeting CBLB as a potential therapeutic approach for disseminated candidiasis. Nat. Med 22: 906–914. [PubMed: 27428899]
39. Conti HR, Huppler AR, Whibley N, and Gaffen SL 2014 Animal models for candidiasis. Curr. Protoc. Immunol 105:19.6.1–17. doi: 10.1002/0471142735.im1906s105.: 19–17. [PubMed: 24700323]
40. Zhao Q, Wang X, Nelin LD, Yao Y, Matta R, Manson ME, Baliga RS, Meng X, Smith CV, Bauer JA, Chang CH, and Liu Y 2006 MAP kinase phosphatase 1 controls innate immune responses and suppresses endotoxic shock. J. Exp. Med 203: 131–140. [PubMed: 16380513]
41. Pulli B, Ali M, Forghani R, Schob S, Hsieh KL, Wojtkiewicz G, Linnoila JJ, and Chen JW 2013 Measuring myeloperoxidase activity in biological samples. PLoS. One. 8: e67976. [PubMed: 23861842]
42. Gross S, Gammon ST, Moss BL, Rauch D, Harding J, Heinecke JW, Ratner L, and Piwnica-Worms D 2009 Bioluminescence imaging of myeloperoxidase activity in vivo. Nat. Med 15: 455–461. [PubMed: 19305414]
43. Gabig TG 1983 The NADPH-dependent O-.2-generating oxidase from human neutrophils. J. Biol. Chem 258: 6352–6356. [PubMed: 6304036]
44. Wang X, Meng X, Kuhlman JR, Nelin LD, Nicol KK, English BK, and Liu Y 2007 Knockout of Mkp-1 enhances the host inflammatory responses to Gram-positive bacteria. J. Immunol 178: 5312–5320. [PubMed: 17404316]
45. Wang X, Zhao Q, Matta R, Meng X, Liu X, Liu CG, Nelin LD, and Liu Y 2009 Inducible nitric-oxide synthase expression is regulated by mitogen-activated protein kinase phosphatase-1. J. Biol. Chem 284: 27123–27134. [PubMed: 19651781]
46. Horwood NJ, Page TH, McDaid JP, Palmer CD, Campbell J, Mahon T, Brennan FM, Webster D, and Foxwell BM 2006 Bruton's tyrosine kinase is required for TLR2 and TLR4-induced TNF, but not IL-6, production. J. Immunol 176: 3635–3641. [PubMed: 16517732]
47. Rossa C, Ehmann K, Liu M, Patil C, and Kirkwood KL 2006 MKK3/6-p38 MAPK signaling is required for IL-1beta and TNF-alpha-induced RANKL expression in bone marrow stromal cells. J. Interferon Cytokine Res 26: 719–729. [PubMed: 17032166]
48. Frazier WJ, Wang X, Wancket LM, Li XA, Meng X, Nelin LD, Cato AC, and Liu Y 2009 Increased inflammation, impaired bacterial clearance, and metabolic disruption after gram-negative sepsis in Mkp-1-deficient mice. J. Immunol 183: 7411–7419. [PubMed: 19890037]
49. Nourshargh S, and Alon R 2014 Leukocyte migration into inflamed tissues. Immunity. 20;41: 694–707.
50. Brown GD 2011 Innate antifungal immunity: the key role of phagocytes. Annu. Rev. Immunol 29:1–21. doi: 10.1146/annurev-immunol-030409-101229.: 1–21. [PubMed: 20936972]
51. Vonk AG, Netea MG, van der Meer JW, and Kullberg BJ 2006 Host defence against disseminated Candida albicans infection and implications for antifungal immunotherapy. Expert. Opin. Biol. Ther 6: 891–903. [PubMed: 16918256]
52. Louie A, Baltch AL, Smith RP, Franke MA, Ritz WJ, Singh JK, and Gordon MA 1994 Tumor necrosis factor alpha has a protective role in a murine model of systemic candidiasis. Infect. Immun 62: 2761–2772. [PubMed: 8005666]
53. Steinshamn S, and Waage A 1992 Tumor necrosis factor and interleukin-6 in Candida albicans infection in normal and granulocytopenic mice. Infect. Immun 60: 4003–4008. [PubMed: 1398912]
54. Djeu JY, Blanchard DK, Halkias D, and Friedman H 1986 Growth inhibition of Candida albicans by human polymorphonuclear neutrophils: activation by interferon-gamma and tumor necrosis factor. J. Immunol 137: 2980–2984. [PubMed: 3093587]

55. Aratani Y, Kura F, Watanabe H, Akagawa H, Takano Y, Suzuki K, Dinauer MC, Maeda N, and Koyama H 2002 Relative contributions of myeloperoxidase and NADPH-oxidase to the early host defense against pulmonary infections with Candida albicans and Aspergillus fumigatus. Med. Mycol 40: 557–563. [PubMed: 12521119]
56. Klebanoff SJ 2005 Myeloperoxidase: friend and foe. J. Leukoc. Biol 77: 598–625. [PubMed: 15689384]
57. Yu L, Quinn MT, Cross AR, and Dinauer MC 1998 Gp91(phox) is the heme binding subunit of the superoxide-generating NADPH oxidase. Proc. Natl. Acad. Sci. U. S. A 95: 7993–7998. [PubMed: 9653128]
58. Peng T, Lu X, and Feng Q 2005 Pivotal role of gp91phox-containing NADH oxidase in lipopolysaccharide-induced tumor necrosis factor-alpha expression and myocardial depression. Circulation 111: 1637–1644. [PubMed: 15795323]
59. El BJ, Faust RP, Johnson JL, and Babior BM 1996 Phosphorylation of the respiratory burst oxidase subunit p47phox as determined by two-dimensional phosphopeptide mapping. Phosphorylation by protein kinase C, protein kinase A, and a mitogen-activated protein kinase. J. Biol. Chem 271: 6374–6378. [PubMed: 8626435]
60. Brown GD, Herre J, Williams DL, Willment JA, Marshall AS, and Gordon S 2003 Dectin-1 mediates the biological effects of beta-glucans. J. Exp. Med 197: 1119–1124. [PubMed: 12719478]
61. Gantner BN, Simmons RM, Canavera SJ, Akira S, and Underhill DM 2003 Collaborative induction of inflammatory responses by dectin-1 and Toll-like receptor 2. J. Exp. Med 197: 1107–1117. [PubMed: 12719479]
62. Endo D, Fujimoto K, Hirose R, Yamanaka H, Homme M, Ishibashi KI, Miura N, Ohno N, and Aratani Y 2017 Genetic Phagocyte NADPH Oxidase Deficiency Enhances Nonviable Candida albicans-Induced Inflammation in Mouse Lungs. Inflammation. 40: 123–135. [PubMed: 27785664]
63. Rouse J, Cohen P, Trigon S, Morange M, Alonso-Llamazares A, Zamanillo D, Hunt T, and Nebreda AR 1994 A novel kinase cascade triggered by stress and heat shock that stimulates MAPKAP kinase-2 and phosphorylation of the small heat shock proteins. Cell 78: 1027–1037. [PubMed: 7923353]
64. Kotlyarov A, Neininger A, Schubert C, Eckert R, Birchmeier C, Volk HD, and Gaestel M 1999 MAPKAP kinase 2 is essential for LPS-induced TNF-alpha biosynthesis. Nat. Cell Biol 1: 94–97. [PubMed: 10559880]
65. Liu Y, Shepherd EG, and Nelin LD 2007 MAPK phosphatases - regulating the immune response. Nat. Rev. Immunol 7: 202–212. [PubMed: 17318231]
66. Tiedje C, Holtmann H, and Gaestel M 2014 The role of mammalian MAPK signaling in regulation of cytokine mRNA stability and translation. J. Interferon Cytokine Res 34: 220–232. [PubMed: 24697200]
67. Tsang E, Giannetti AM, Shaw D, Dinh M, Tse JK, Gandhi S, Ho H, Wang S, Papp E, and Bradshaw JM 2008 Molecular mechanism of the Syk activation switch. J. Biol. Chem 283: 32650–32659. [PubMed: 18818202]
68. Roos D, Kuhns DB, Maddalena A, Bustamante J, Kannengiesser C, de BM, van LK, Koker MY, Wolach B, Roesler J, Malech HL, Holland SM, Gallin JI, and Stasia MJ 2010 Hematologically important mutations: the autosomal recessive forms of chronic granulomatous disease (second update). Blood Cells Mol. Dis 44: 291–299. [PubMed: 20167518]
69. Griffith CE, Zhang W, and Wange RL 1998 ZAP-70-dependent and -independent activation of Erk in Jurkat T cells. Differences in signaling induced by H2o2 and Cd3 cross-linking. J. Biol. Chem 273: 10771–10776. [PubMed: 9553143]
70. Pricop L, Gokhale J, Redecha P, Ng SC, and Salmon JE 1999 Reactive oxygen intermediates enhance Fc gamma receptor signaling and amplify phagocytic capacity. J. Immunol 162: 7041–7048. [PubMed: 10358146]
71. Zent R, Ailenberg M, Downey GP, and Silverman M 1999 ROS stimulate reorganization of mesangial cell-collagen gels by tyrosine kinase signaling. Am. J. Physiol 276: F278–F287. [PubMed: 9950959]

72. Sakai J, Li J, Subramanian KK, Mondal S, Bajrami B, Hattori H, Jia Y, Dickinson BC, Zhong J, Ye K, Chang CJ, Ho YS, Zhou J, and Luo HR 2012 Reactive oxygen species-induced actin glutathionylation controls actin dynamics in neutrophils. Immunity 37: 1037–1049. [PubMed: 23159440]

73. Hunter T 1995 Protein kinases and phosphatases: the yin and yang of protein phosphorylation and signaling. Cell 80: 225–236. [PubMed: 7834742]

74. Keyse SM 1998 Protein phosphatases and the regulation of MAP kinase activity. Semin. Cell Dev. Biol 9: 143–152. [PubMed: 9599409]

75. Denu JM, and Dixon JE 1998 Protein tyrosine phosphatases: mechanisms of catalysis and regulation. Curr. Opin. Chem Biol 2: 633–641. [PubMed: 9818190]

76. Nathan C, and Shiloh MU 2000 Reactive oxygen and nitrogen intermediates in the relationship between mammalian hosts and microbial pathogens. Proc. Natl. Acad. Sci. U. S. A 97: 8841–8848. [PubMed: 10922044]

Key Points

- *Gsr*$^{-/-}$ mice exhibited markedly increased susceptibility to *C. albicans* challenge.
- *Gsr*$^{-/-}$ neutrophils display defects in fungicidal activity.
- *Gsr*$^{-/-}$ macrophages exhibit an enhanced inflammatory response.

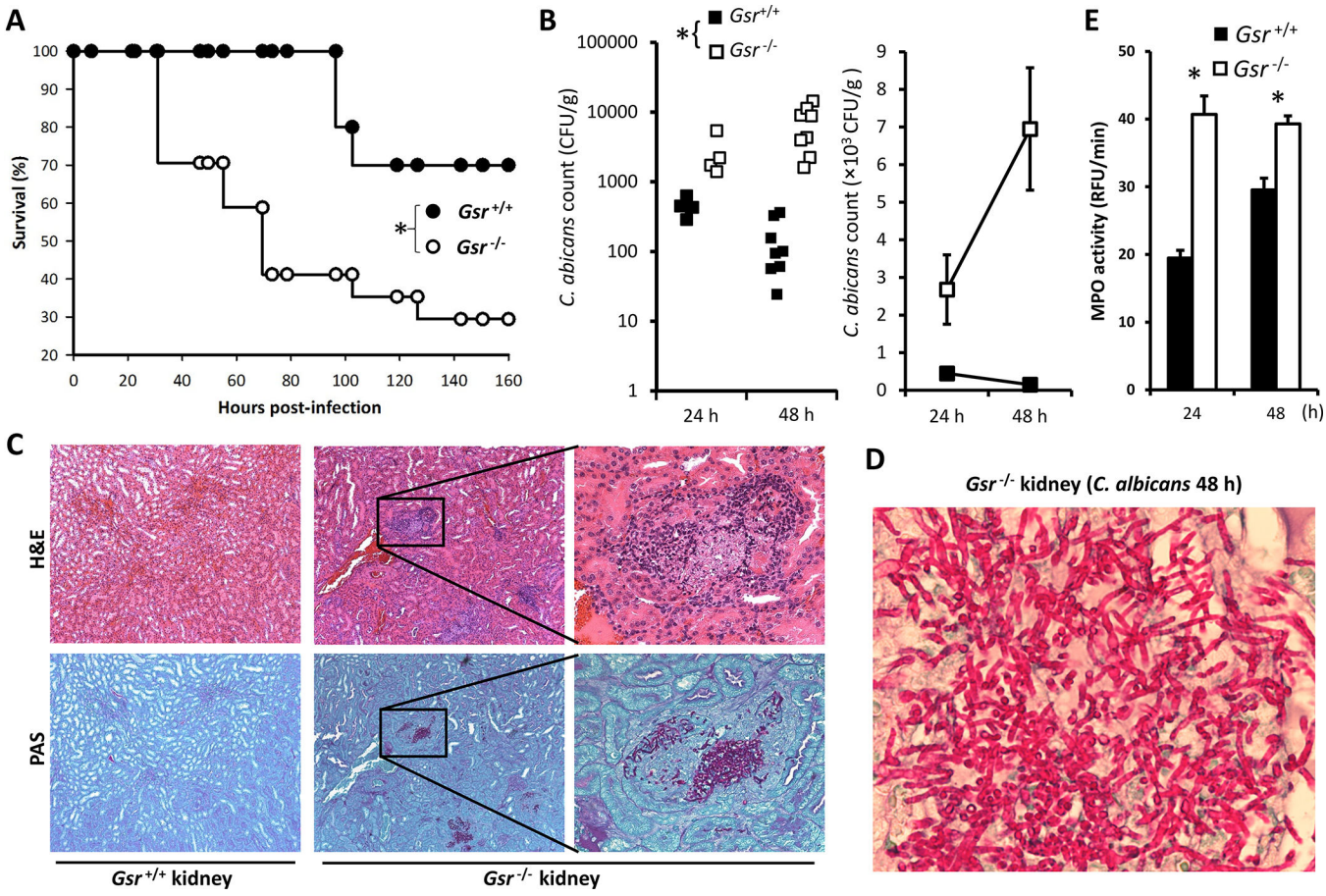

Figure 1. Survival curve and kidney sections of WT and *Gsr*$^{-/-}$ mice after *C. albicans* challenge.

Mice were infected *i.v.* with 5×10^5 CFU of *C. albicans* (SC5314). **A.** Survival curve of WT and *Gsr*$^{-/-}$ mice. *, $p<0.05$ (Kaplan-Meier's Log-Rank test). $n_{WT}=10$; $n_{Gsr^{-/-}}=17$. **B.** Kidney fungal burden in WT and *Gsr*$^{-/-}$ mice. WT and *Gsr*$^{-/-}$ mice were infected *i.v.* with 5×10^5 CFU of *C. albicans* and sacrificed 24 or 48 h later to harvest kidneys for the assessment of fungal burdens by culture. *, $p<0.05$ (t-test). Graph on the right depicts the dramatic contrast between the decline and increase in fungal burden in WT and *Gsr*$^{-/-}$ mice, respectively. **C.** H&E and PAS stained kidney sections. Kidney tissues were harvested 48 h post infection. Adjacent sections were stained with H&E and PAS. **D.** A high resolution image of fungal lesion in the kidney section of a *C. albicans*-infected *Gsr*$^{-/-}$ mouse after PAS staining. **E.** MPO activity in kidney homogenates. MPO activity was assayed using ADHP and H_2O_2 as substrates through measuring the kinetics of fluorescence (ex 535 nm/em 590 nm).

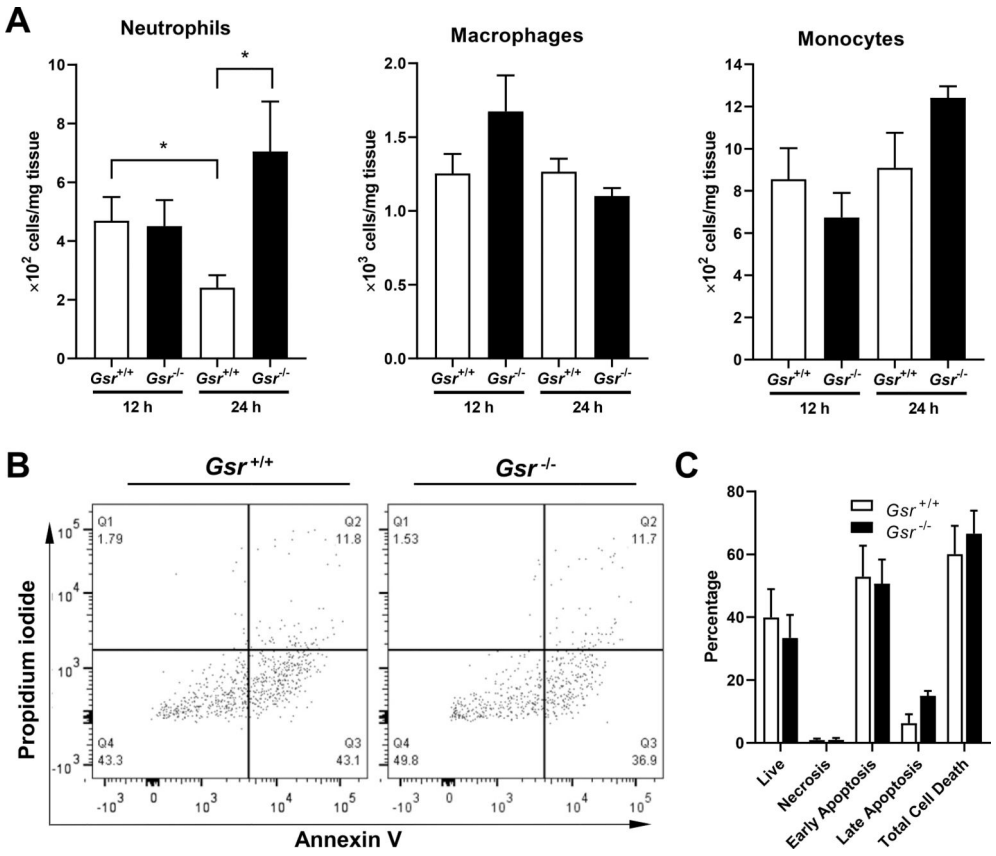

Figure 2.

Leukocyte numbers and neutrophil viability in the kidneys of C. albicans-infected *Gsr*$^{+/+}$ and *Gsr*$^{-/-}$ mice. Mice were infected *i.v.* with 5×10^5 CFU of *C. albicans* (SC5314) and then sacrificed at the indicated time to isolate kidneys. Leukocytes were enriched through Percoll gradient centrifugation, counted, and stained with different leukocyte markers for flow cytometry. Cells were first gated on forward scatter (FSC) and side scatter (SSC) to exclude cell debris, and viable cells were then gated for CD45$^+$CD11b$^+$Ly6G$^+$F4/80$^-$ neutrophils, CD45$^+$CD11b$^+$Ly6C^{hi} monocytes, and CD45$^+$CD11b$^+$F4/80$^+$ macrophages. **A.** Numbers of neutrophils, macrophages, and monocytes in the kidneys at 12 and 24 h post *C. albicans* infection. Values represent means±SE (n=4–5). *, p<0.05 (Two-way ANOVA). **B.** Representative annexin V-Alexa 488 vs PI contour plots. Leukocytes were enriched from enzymatically digested kidneys from *Gsr*$^{+/+}$ or *Gsr*$^{-/-}$ mice 24 h post *C. albicans* infection. These cells were then stained with CD45, Ly6G, annexin V, and PI, and subsequently assessed by flow cytometry. Neutrophils were gated as CD45+Ly6G+ cells, and further divided as necrotic (PI$^+$), early apoptotic (annexin V$^+$), late apoptotic (annexin V$^+$ PI$^+$), and live cells (annexin V$^-$PI$^-$). **C.** Percentage of live, necrotic, early apoptotic, late apoptotic, and total dead cells. Values represent means±SE (n=4–5).

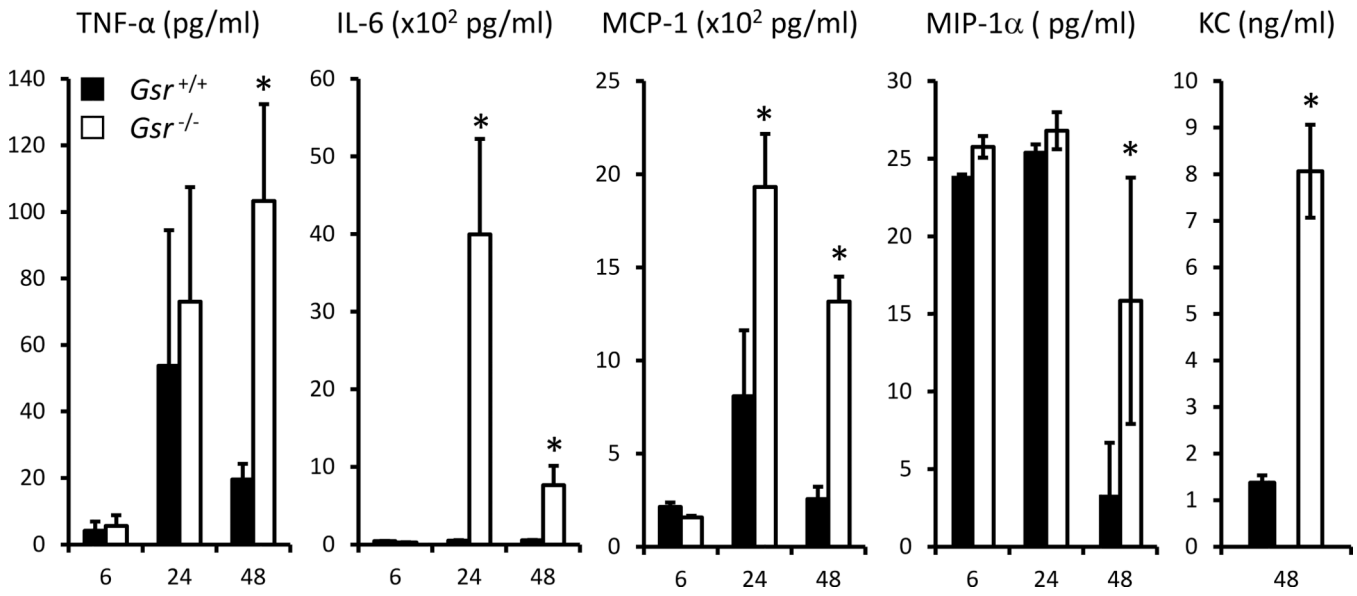

Figure 3. Gsr deletion results in exaggerated inflammatory response following *C. albicans* infection.

WT and $Gsr^{-/-}$ mice were infected *i.v.* with 5×10^5 CFU of *C. albicans*. Mice were sacrificed 6, 24, or 48 hours later to harvest blood for assessment of blood cytokines by ELISA. Values are means ± SE. *, $p<0.05$ (t-test, n=4).

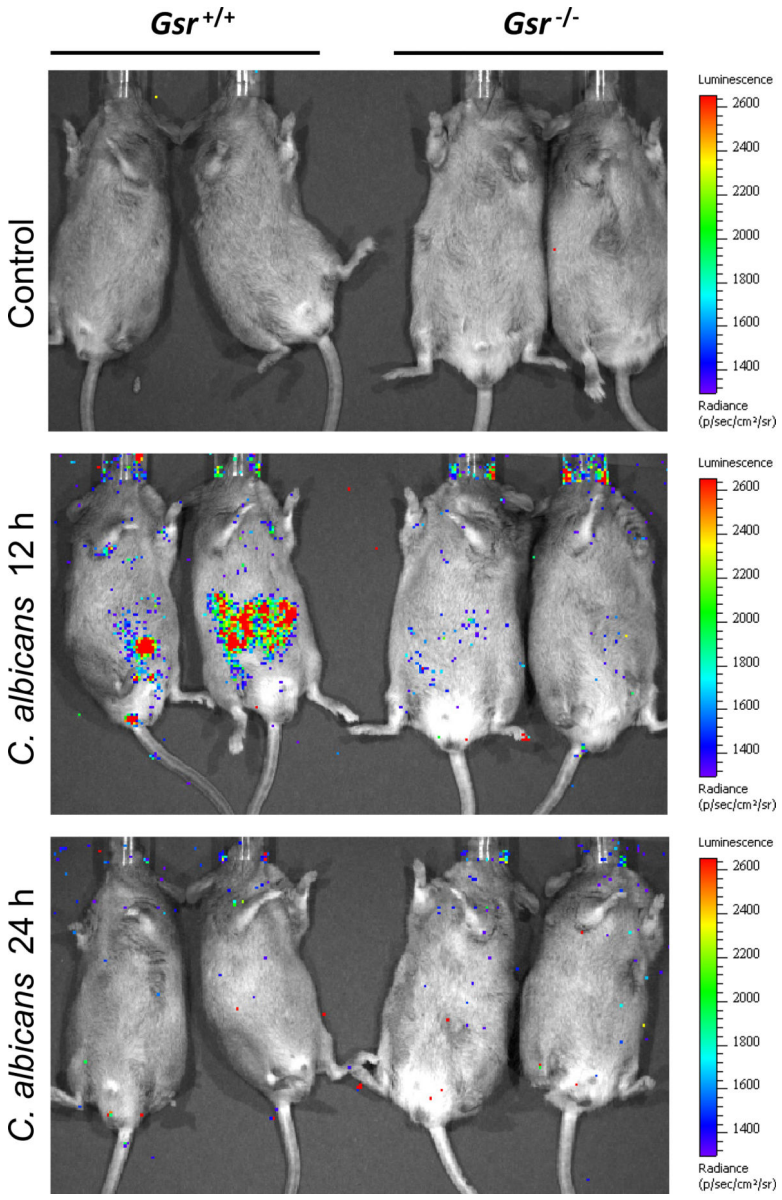

Figure 4. Gsr deficiency leads to diminished respiratory burst activity in *C. albicans*-infected mice.

The respiratory burst burst activity *in vivo* in *C. albicans*-challenged mice (5×10^5 CFU i.v. per mouse) was detected by luminol bioluminescence. Uninfected (control) or *C. albicans*-infected mice (12 or 24 h post challenge) were administered luminol (200 μg/g b.w.) to collect luminescent images (exposure time, 5 min; FOV, D; binning, 8). Images were from a representative experiment.

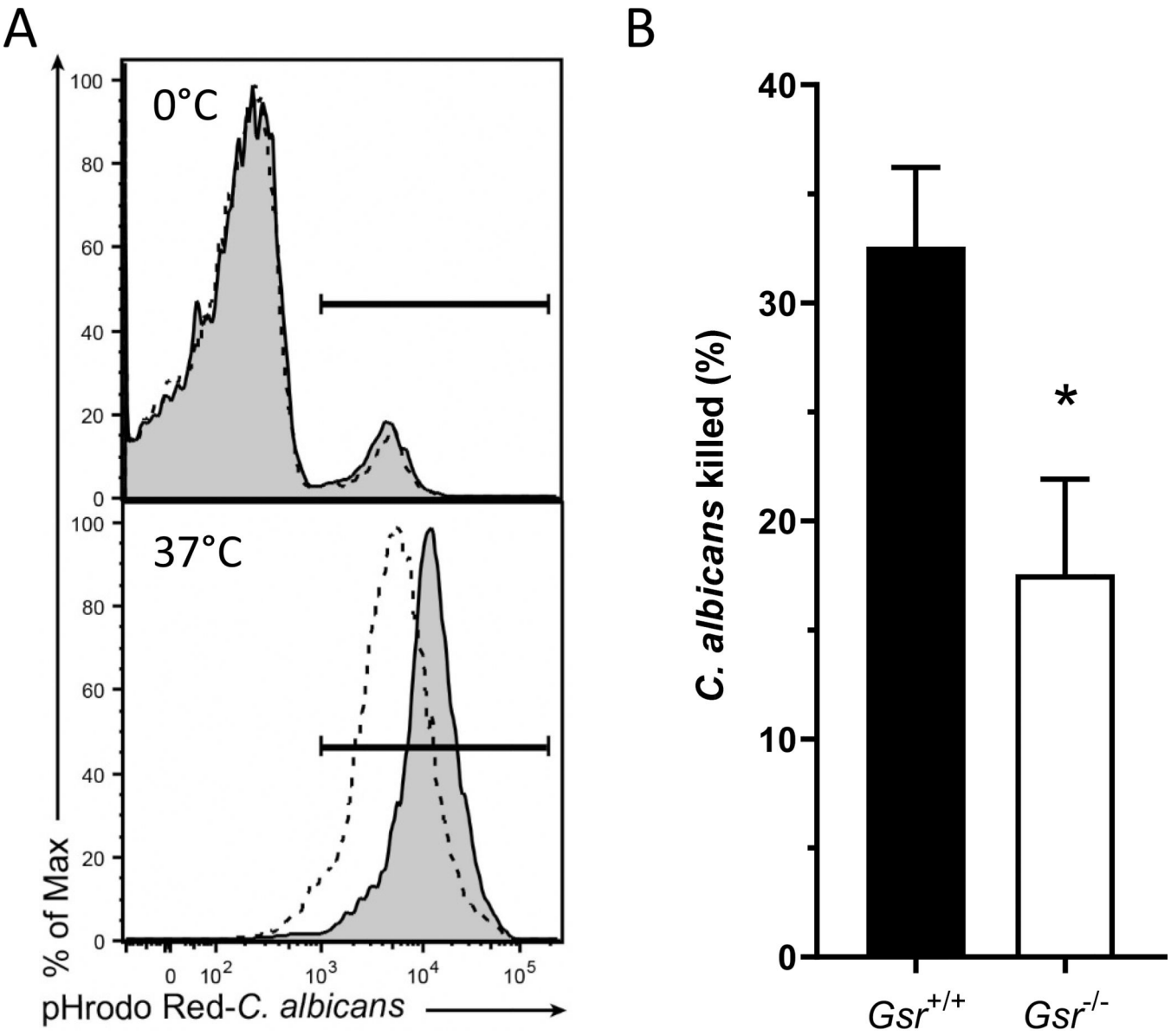

Figure 5. *Gsr* deletion results in compromised yeast phagocytosis by neutrophils.

A. Phagocytosis of *C. albicans* by WT and $Gsr^{-/-}$ neutrophils. Purified BM neutrophils were incubated with pHrodo red-tagged *C. albicans* (MOI=10) at 0°C or 37°C for 30 min, and then labeled with Ly6G–Pacific Blue on ice for 20 min. Cells were subsequently washed twice with cold FACS buffer and analyzed by flow cytometry. $Ly6G^+$ neutrophils cells were analyzed for the presence of pHrodo red-tagged *C. albicans.* Solid lines depict $Gsr^{+/+}$ and dashed lines depict $Gsr^{-/-}$ neutrophils. **B.** Fungal killing assays. Serum-opsonized *C. albicans* yeast were incubated with either purified BM neutrophils or medium for 60 min at an MOI of 10:1, and then the neutrophils were lyzed by hypo-osmolarity. The mixtures were then serially diluted, and plated onto YPD agar plates to culture at 37°C for approximately 24 h. Viable *C. albicans* cells were scored by counting the colonies formed on the YPD plates. The percentage of killing was calculated using the medium-treated *C. albicans* as references. Values are means ± SE. *, $p<0.05$ (t-test, n=3).

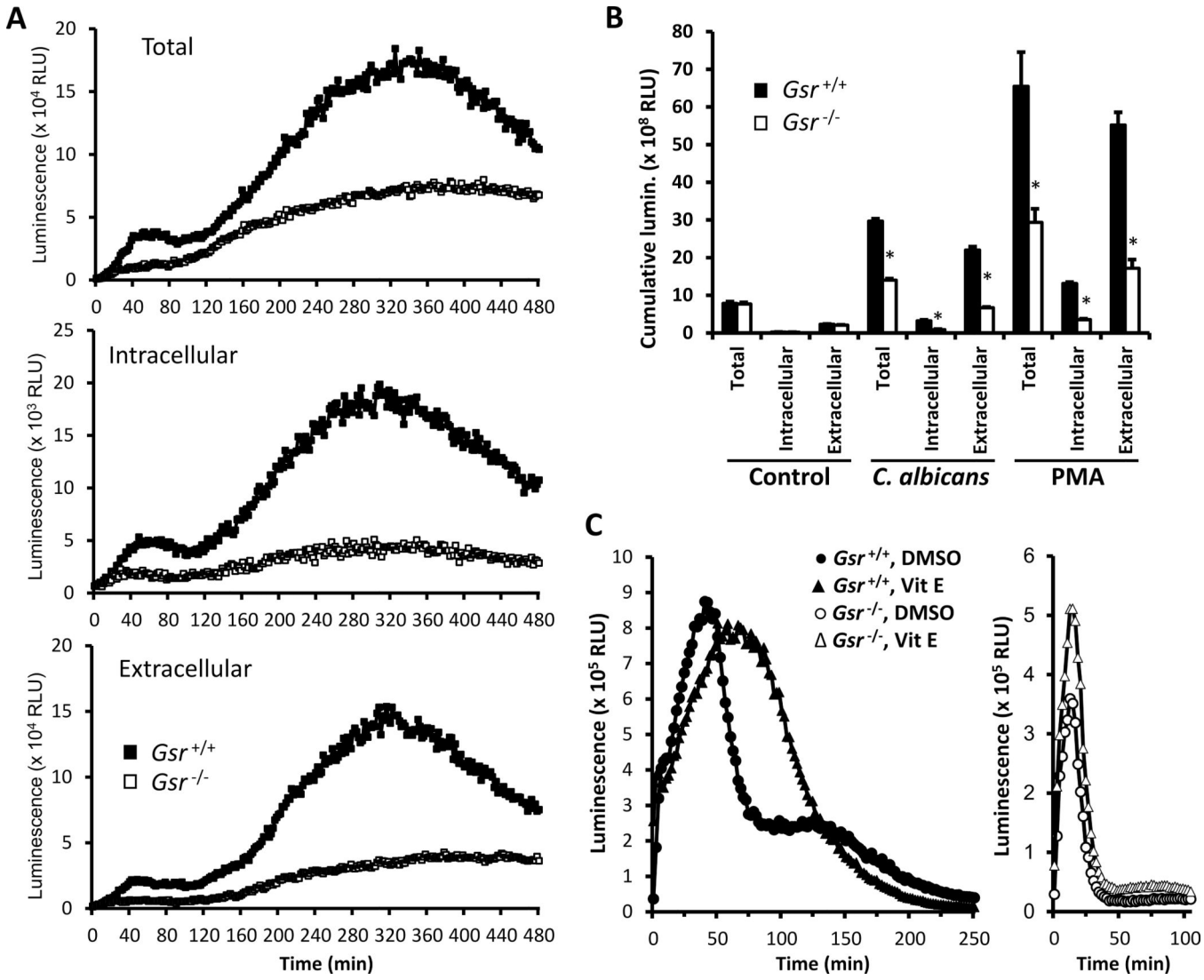

Figure 6. *Gsr* deletion impairs respiratory burst of neutrophils.

Purified BM neutrophils were stimulated with heat-killed *C. albicans* (MOI=10) or PMA (0.5 μM). Respiratory burst was measured using luminol or isoluminol in the presence or absence of SOD and catalase in 96-well plates in a Biotek Synergy 2 luminometer. **A.** Top: kinetics of total respiratory burst activity. Middle: kinetics of intracellular respiratory burst activity. Bottom: kinetics of extracellular burst activity. Values represent the means. Differences between $Gsr^{+/+}$ and $Gsr^{-/-}$ are significant ($p<0.05$, two-way ANOVA, n=4). **B.** Cumulative respiratory burst activity over 8 h. Values are means±SE. *, $p<0.05$ (t-test, n=4). **C.** PMA-stimulated PMN respiratory burst of $Gsr^{+/+}$ (*Left*) and $Gsr^{-/-}$ (*Right*) with the presence (▲ or △) and absence (● or ○) of vitamin E (0.2 mM), measured using luminol.

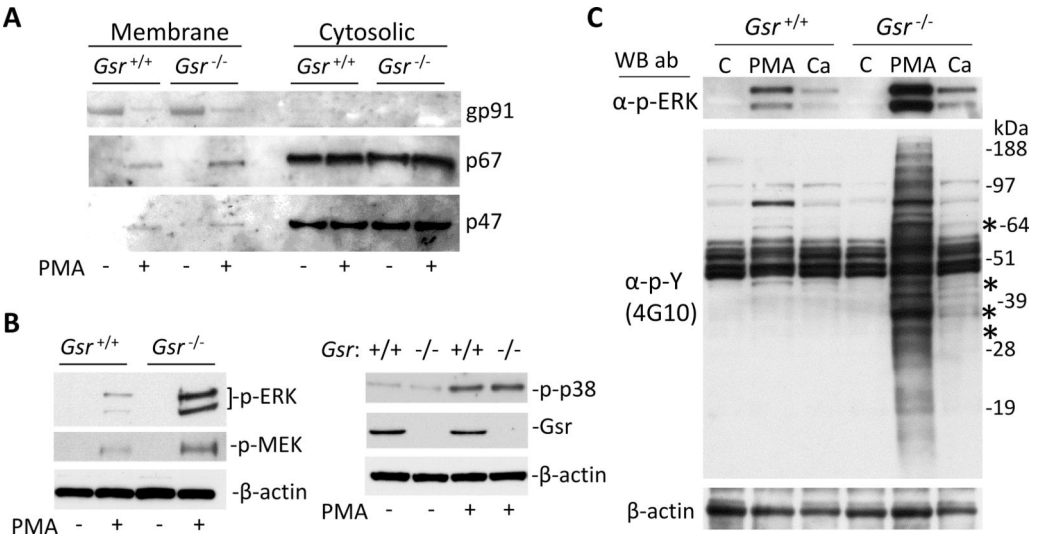

Figure 7. Assembly of NADPH oxidase complexes, ERK and p38 activation, and tyrosine phosphorylation after stimulation in wildtype and *Gsr*$^{-/-}$ neutrophils.

A. Subcellular localization of different NADPH oxidase subunits in WT and *Gsr*$^{-/-}$ neutrophils before and after PMA stimulation. Purified WT and *Gsr*$^{-/-}$ neutrophils were stimulated with 0.5 μM PMA for 15 min or left unstimulated. Cells were lysed and fractionated into cytosolic and membrane fractions by ultracentrifugation. The subcellular fractions were subjected to Western blot analyses, using Abs against gp91^{phox}, p47^{phox}, and p67^{phox} subunits of the NADPH oxidase. **B.** ERK and p38 activities in control and PMA-stimulated neutrophils. Purified WT and *Gsr*$^{-/-}$ neutrophils were stimulated with 0.5 μM PMA for 15 min or left unstimulated, and lysed. Cell lysates were subjected to Western blot analysis using Abs against phospho-ERK, phospho-MEK, phospho-p38, and Gsr. Blots were stripped and probed with a mAb against β-actin to verify comparable protein loading. **C.** Differential tyrosine phosphorylation and ERK activation in WT and *Gsr*$^{-/-}$ neutrophils following PMA and *C. albicans* stimulation. Purified BM neutrophils were stimulated with 0.5 μM PMA for 30 min, or with heat-killed *C. albicans* yeast (MOI=5) for 60 min, or left unstimulated. Neutrophils were lysed and cell lysates were subject to Western blot analysis using an Ab against phospho-ERK or phosphotyrosine (4G10). A blot was stripped and reprobed with a mAb against β-actin. The positions of molecular mass markers were shown on the right side of the blot. Asterisks indicate several tyrosine phosphorylated proteins in *C. albicans*-stimulated neutrophils.

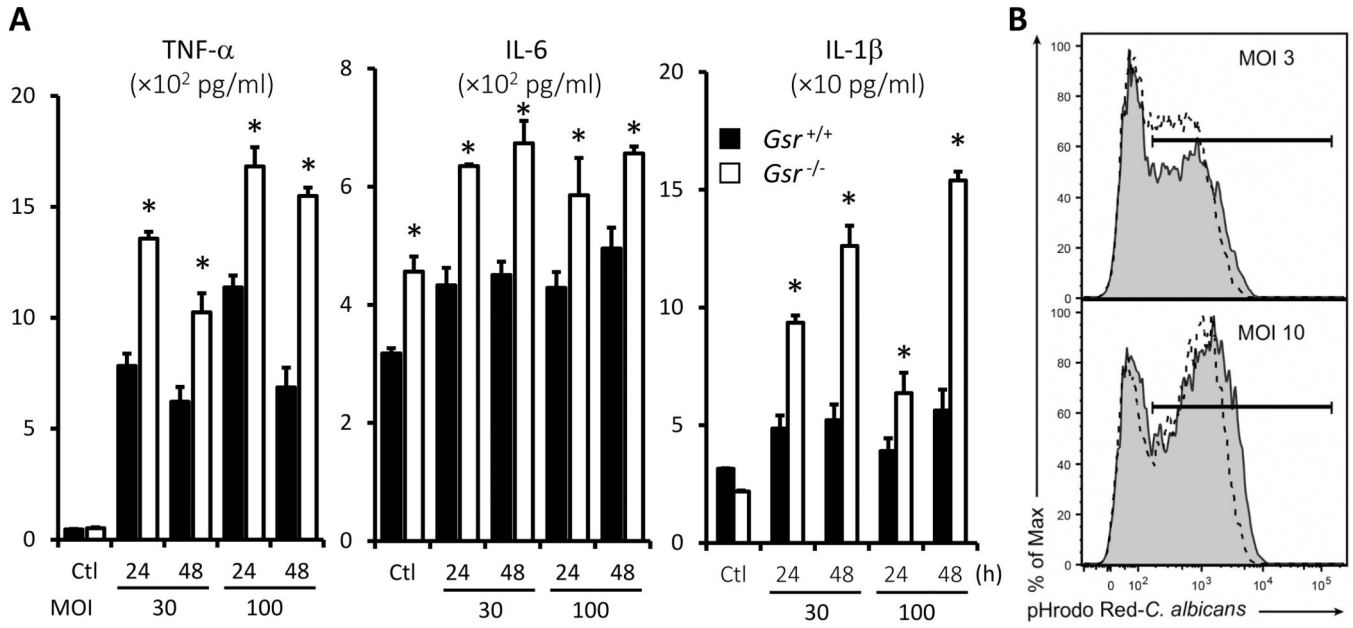

Figure 8. Gsr deletion in macrophages results in exaggerated cytokine production following *C. albicans* stimulation with little effect on macrophage phagocytic activity.

A. *C. albicans*-induced cytokine production by WT and $Gsr^{-/-}$ macrophages. WT and $Gsr^{-/-}$ BMDM were stimulated with heat-killed *C. albicans* (MOI=30, 100) for 24 or 48 h, and cytokines in the medium were quantified by ELISA. *, $p<0.05$ (t-test, n=4). **B.** Phagocytosis of *C. albicans* by WT and $Gsr^{-/-}$ BMDM. WT and $Gsr^{-/-}$ BMDM were incubated with pHrodo red-tagged *C. albicans* (MOI= 3 or 10) at 37°C for 30 min, and then labeled with Pacific blue-labelled anti-mouse F4/80 on ice for 10 min. Cells were subsequently washed twice with cold FACS buffer and analyzed by flow cytometry. $F4/80^+$ BMDM were analyzed for the presence of pHrodo red-tagged *C. albicans.* Solid lines depict $Gsr^{+/+}$ and dashed lines depict $Gsr^{-/-}$ cells.

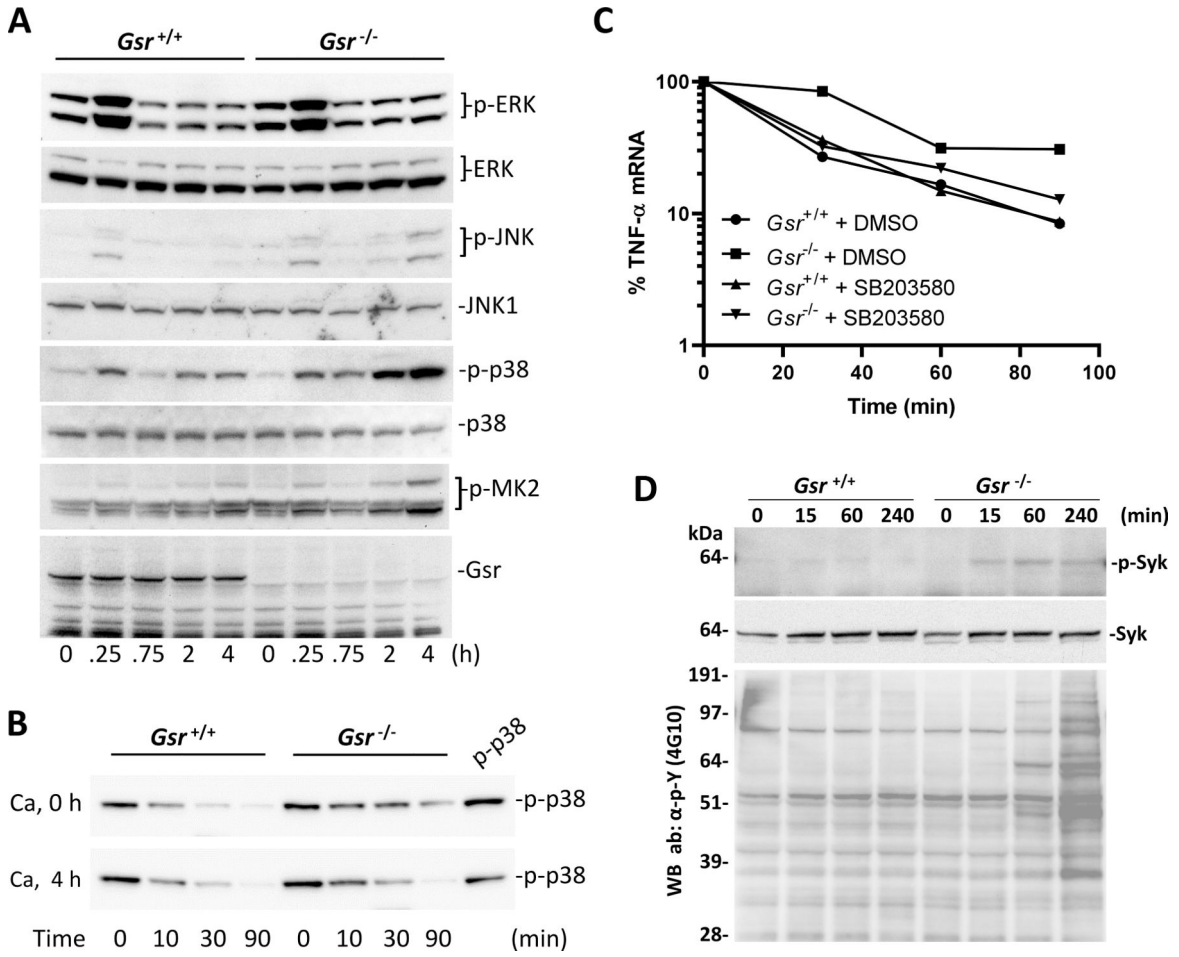

Figure 9. *C. albicans*-stimulated *Gsr*$^{-/-}$ BMDM exhibit augmented p38, JNK, and Syk activities, attenuated Mkp-1 activity, and enhanced TNF-α mRNA stability.

A. The kinetics of ERK, JNK, and p38 activation following *C. albicans* stimulation. WT and *Gsr*$^{-/-}$ BMDM were stimulated with heat-killed *C. albicans* (MOI=5) for the indicated lengths of time, and harvested. Cell lysates were subjected to Western blot analysis using Abs against total or phospho-specific protein kinases. The blot was stripped and blotted with a rabbit Ab against Gsr. **B.** Dephosphorylation of phospho-p38 by Mkp-1 immunoprecipitated from WT and *Gsr*$^{-/-}$ BMDM. BMDM (10^7 cells) were either left untreated (*Upper panel*) or stimulated with heat-killed *C. albicans* for 4 h (*Lower panel*). Cells were lysed and Mkp-1 was immunoprecipitated using protein A-Sepharose beads and polyclonal Abs against Mkp-1. The immunoprecipitates were then incubated with recombinant phospho-p38 for different times. The reaction was stopped and the mixtures were resolved using 10% NuPAGE gels. The same amount of phospho-p38 was run on the right side as a positive control. Western blot analysis was performed using a phospho-p38-specific Ab. Ca, *C. albicans*. **C.** p38-dependent increase in TNF-α mRNA stability in *C. albicans*-stimulated *Gsr*$^{-/-}$ BMDM. BMDM were stimulated with heat-killed *C. albicans* (MOI=5) for 5.5 h, and then treated with DMSO or 10 μ SB203580 for 30 min. Subsequently, cells were treated with actinomycin D (5 μg/ml) for different times to isolate total RNA. TNF-α mRNA levels were assessed by qRT-PCR and normalized to 18s. TNF-α

mRNA levels at time 0 were set as 100%. Results from a representative experiment are shown. **D.** Augmented Syk activity and global tyrosine phosphorylation in *Gsr*$^{-/-}$ BMDM following hypha stimulation. WT and *Gsr*$^{-/-}$ BMDM were stimulated with heat-killed *C. albicans* hyphae (MOI=5) for the indicated lengths of time, and harvested. Cell lysates were subjected to Western blot analysis using a polyclonal Ab against phospho-Syk (*Upper panel*), a mouse mAb against total Syk (*Middle panel*), and the 4G10 mAb against phosphotyrosine (*Lower panel*). The positions of the molecular mass standards were marked on the left of the blots.